COWRIE-EMF-01-2002

A BASELINE ASSESSMENT OF ELECTROMAGNETIC FIELDS GENERATED BY OFFSHORE WINDFARM CABLES

FINAL REPORT

PREPARED BY:

CENTRE FOR MARINE AND COASTAL STUDIES

CENTRE FOR INTELLIGENT MONITORING SYSTEMS

APPLIED ECOLOGY RESEARCH GROUP

(All University *of* Liverpool)

&

ECONNECT LTD

JULY 2003
J2733/V1/07-03

This report has been commissioned by COWRIE

Centre for Marine and Coastal Studies
University of Liverpool
Vanguard Way
Birkenhead CH41 9HX

Tel: 0151 650 2275
Fax: 0151 650 2274
E-mail: ahough@liv.ac.uk

This report has been prepared by CMACS for COWRIE as part of the generic research programme identified to benefit the offshore windfarm industry. The views and recommendations presented in this report are not necessarily those of COWRIE, its individual members, or the organisations they represent, who accordingly have no legal liability for its contents.

CMACS (2003) A baseline assessment of electromagnetic fields generated by offshore windfarm cables. COWRIE Report EMF - 01-2002 66.

EXECUTIVE SUMMARY

COWRIE identified as priority research the issue of electromagnetic fields (EMF) generated by offshore windfarm power cables and their possible effect on organisms that are sensitive to these fields. A consortium, lead by CMACS, was contracted to carry out a Stage 1 investigation to investigate the following:

- The likely EMF emitted from a subsea power cable.
- A suggested method to measure EMF in the field, which could be applied by windfarm developers or in future projects.
- Guidance on mitigation measures to reduce EMF.
- Consideration of the results for the next stage of investigation into the effects of EMF on electro-sensitive species.

An assessment of existing publications (both hard and electronic) and direct communications regarding EMF emitted by undersea power cables suggested that the current state of knowledge is too variable and inconclusive to make an informed assessment of any possible environmental impact of EMF in the range of values likely to be detected by organisms sensitive to electric and magnetic fields. Therefore modelling and direct measurement of the electric and magnetic field components of EMF was undertaken.

An Alternating Current (AC) Conduction Field Solver model and Eddy Current Field Solver model were used within the 'Maxwell 2D' software program which allows the simulation of electromagnetic and electrostatic fields in structures with uniform cross-sections by solving Maxwell's equations using the finite-element method. The modelling was based on EMF generated by a 132kV XLPE three-phase submarine cable designed by Pirelli with an AC current of 350 amps buried at a depth of 1m.

The results of the model simulations showed that a cable with perfect shielding i.e. where conductor sheathes are grounded, does not generate an electric field (E-field) directly. However, a magnetic field (B-field) is generated in the local environment by the alternating current in the cable. This in turn, generates an induced E-field close to the cable within the range detectable by electro-sensitive fish species. Simulations with non-perfect shielding, i.e. where there is poor grounding of sheathes, showed that there is a leakage E-field, but it is smaller than the induced E-fields and unlikely to be additive.

A method is provided for calculating the induced E-field around a low frequency AC power cable due to the emanating B-field. This method requires *in situ* measurement of the B-field generated by an operational cable.

To consider mitigation, the models simulated changes in permeability of the power cable armour and conductivity of the cable sheath and armour. The model predicted that as the permeability of the armour increased the resultant EMF strength outside the cable decreased. The model also showed that a non-linear relationship exists between electromagnetic field strength adjacent to the cable and permeability of the armouring material. This indicated that using materials with very high permeability values for armouring of submarine power cables could help to reduce the EMF generated to below the lowest known level that electroreceptive elasmobranchs can detect. As the conductivity of the armour was increased the model showed that the resultant EMF strength outside the cable decreased. A linear relationship was found between electromagnetic field strength and the conductivity of the materials used in the cable. These results indicate that a reduction in the strength of the electromagnetic fields induced by a three-phase 132kV XLPE submarine cable can be achieved through the application of materials with high conductivity and high permeability. These results provide useful information for consideration during the design and manufacture of submarine cables with reduced EMF emissions.

Burial was shown to be ineffective in 'dampening' the B-field, however cable burial to a depth of at least 1m is likely to provide some mitigation for the possible impacts of the strongest B-field and induced E-fields (that exist within millimetres of the cable) on sensitive fish species, owing to the physical barrier of the substratum.

An additional mitigation consideration is the use of substations to convert the voltage from 33kV to 132kV would reduce the current carried by a cable and would therefore reduce the induced E-fields by a factor of four. This could be used to add to mitigation of the EMF effects of sending power to the shore but probably has practical and economic limitations.

In terms of the potential significance of the modelled results to electrosensitive fish the following conclusions were made:

- EMF emitted by an industry standard three-core power cable will induce E-fields.
- In the case modelled, this resulted in a predicted E-field of approximately 91μV/m (=0.9 μV/cm) in seawater above a cable buried to 1m. This level of E-field is on the boundary of E-field emissions that are expected to attract and those that repel elasmobranchs (the most widespread electrosensitive fish group of UK coastal waters).
- In addition, the induced E-fields calculated from the B-fields measured *in situ* were also within the lower range of detection by elasmobranchs.

- The options for mitigation using either changes in permeability or conductivity indicate that the induced E-field can be effectively reduced. However, unless highly specialised materials and manufacturing process are used with high permeability values, the E-field will still remain within the lower range of detection of elasmobranchs. Hence any reduction in E-field emission using existing materials could minimise the potential for an avoidance reaction by a fish if it encountered the field but may still result in an attraction response.
- Another important consideration is the relationship between the amount of cable, either buried or unburied, producing induced E-fields and the available habitat of an electrosensitive species.
- There is also a need to determine if the power cable operating frequency (50Hz) and associated sub-harmonic frequencies have any effect on the EMFs that are detectable by UK electrosensitive fishes.

Finally, a number of further studies are recommended to direct future research to fully understand the interaction of the induced E-fields from subsea power cables with electrosensitive fish and any implications of the B-fields for organisms that rely on a magnetic sense.

CONTENTS

GLOSSARY OF TERMS

RMS	The 'square root of the mean squared' used by engineers to describe levels of alternating signals. ie. Current flow in power cables goes first in one direction then reverses. RMS is the equivalent current flowing in one direction continuously that would supply the same amount of electrical power.

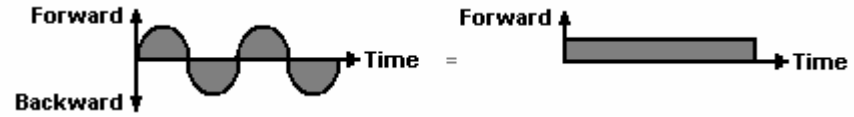

Note: The peak of the alternating signal is typically 1.4 times larger than its RMS value

Voltage	Voltage (V) is a measurement of the electrical potential difference that exists between two points. 1,000,000 μV = 1,000 mV = 1 V
μV	micro-volts
mV	milli-volts
Electric field (**E**)	Electric field (V/m) is a measure of how the voltage changes when a measurement point is moved in a given direction. If no direction is stated then the direction can be assumed to be the one that produces the largest change. 1 μV/cm = 100 μV/m 1,000,000 μV/m = 1000 mV/m = 1 V/m
Current (A)	An electric charge in motion (amps)
AC	Alternating current (or voltage) i.e. flows forward then backwards at 50 times per second (Hz)
DC	Direct current i.e. flows in the same direction all the time. (0 Hz)
Current density	Current density (A/m²) is analogous to water flow. It is a measure of how much electrical current in amps (A) is flowing through a given area.
Magnetic field (**H**)	Magnetic field (A/m) is analogous to water flow. It is directly linked to the magnetic flux density (**B**) that is flowing in a given direction. If no direction is stated then it can be assumed to be the direction that produces the largest the magnetic field. **B** = μ **H**, where μ is the permeability of the material. The SI unit for magnetic flux density B is tesla (T) 1 T = 1 Wb/m² 1,000,000,000 nT = 1,000,000 μT = 1,000 mT = 1 T
nT	Nano-tesla
μT	Micro-tesla
mT	Milli-tesla

The Relationship between of various units at 50 Hz (in air or seawater)

nT (B)	μT (B)	Gauss (B)	A/m (**H**)	Applied Induced **E** field (μV/m)
1	0.001	0.00001	0.000796	0.31
100	0.1	0.001	0.07958	31
125.7	0.1257	0.001257	0.1	39
1000	1	0.01	0.795798	314
1257	1.257	0.01257	1	395
10,000	10	0.1	8.0	3,142
100,000	100	1	79.6	31,416
3,000,000	3000	30	2,387.4	942,478

REPORT STRUCTURE

- Section 1 sets the context of the project.
- Section 2 describes cabling strategies for UK offshore windfarms, existing information on EMF generated by subsea power cables and projects that have been carried out in Europe to date.
- Section 3 describes the modelling of EMF generated by subsea power cables for a typical UK offshore windfarm power-cabling scenario.
- Section 4 describes the development and construction of electric and magnetic field sensors constructed for a preliminary investigation into ***in-situ*** EMF generated by subsea power cables and gives a method by which EMF can be calculated by windfarm developers.
- Section 5 considers possible areas of mitigation for the reduction of EMF.
- Section 6 discusses the results of the studies in the context of electro-sensitive fish species.
- Section 7 makes recommendations for future studies.
- Section 8 gives overall conclusions of the investigation.
- Section 9 provides the cited references in numerical order of use in the text.
- Section 10 has the appendices with details of the people and organisations contacted; electrical circuits for the sensors; and a list of electrosensitive fish species of UK coastal waters.

1. INTRODUCTION

In April 2001, eighteen companies successfully pre-qualified for an option to lease areas of the seabed in UK territorial waters from the Crown Estate for the development of offshore windfarms, the first of their kind in the UK coastal zone.

The financial pre-qualification requirements for these eighteen sites initiated the establishment of a trust fund for the purposes of short to medium term, generic environmental studies to benefit the early stages of the offshore windfarm industry as a whole and provide guidance for future developments. The fund is administered by the COWRIE (Collaborative Offshore Wind Research into the Environment) steering group, which represents the offshore windfarm industry, NGO's, GO's, DTI and statutory conservation agencies.

COWRIE has identified a number of priority areas for generic research. One of these areas is the issue of electromagnetic fields (EMF) generated by offshore windfarm power cables and their possible effect on organisms that are sensitive to these fields.

A consortium of departments of the University of Liverpool and Econnect Ltd., lead by the Centre for Marine and Coastal Studies (CMACS) was contracted by COWRIE to attempt to specifically identify and quantify electromagnetic fields (EMF) generated by offshore windfarm subsea power cables. This research was required as the first stage of studies that aim to provide a more informed and objective assessment of the potential effects of EMF on organisms sensitive to both electric and magnetic fields.

1.1 PROJECT BACKGROUND

A preliminary investigation of the potential impacts of offshore windfarm power cables on electro-sensitive fish was carried out at the University of Liverpool during 2001 for the Countryside Council of Wales[1]. In this investigation, Gill & Taylor[1] investigated the potential effect of EMF predicted to be generated by subsea power cabling upon elasmobranch fishes (sharks, skates and rays). Owing to a paucity of information in the literature they undertook a basic laboratory-based experiment to investigate the response of the dogfish, *Scyliorhinus canicula,* to electric fields (E-fields) generated by a direct current (DC) electrode placed in a seawater tank. Although their investigation was only a pilot study the results were notable in that the dogfish avoided constant E-fields at 1000 micro-volts per metre (µV/m), which were simulating the size of the EMF emission predicted from 150kVcables with a current of 600A. The avoidance response by the dogfish was, however, variable amongst individuals and had a relatively low probability of occurring in the conditions presented in Gill & Taylor's

experiment. Importantly individuals of the same species were attracted to an E-field of 10μV/m at 0.1m from the source which is similar to the bioelectric fields emitted by dogfish prey.

Gill & Taylor made a number of recommendations based on the findings of their preliminary research. These recommendations included the following:

- Electric field research, in particular the quantification of fields within different substrata and *in situ* measurement.
- Further directed biological research, especially focussing on species that use inshore habitats and behavioural responses to E-fields.
- GIS mapping and interrogation, to provide a database that can guide decisions on the location of offshore windpower sites taking into account, amongst other factors the potential conflicts with elasmobranchs and their resource requirements.

The COWRIE steering group recommended a two-stage approach to further research into EMF and its possible ecological impact. Stage 1 required calculation of the EMF generated by power cables at the seabed, an assessment of the effects of burial and/or shielding and some preliminary *in-situ* measurements of EMF generated by an existing subsea power cable. The consortium, lead by CMACS, was contracted to carry out the Stage 1 investigation to meet the following deliverables under this contract:

- The likely EMF emitted from a subsea power cable.
- A suggested method to measure EMF in the field that could be applied by windfarm developers or in future projects.
- Guidance on mitigation measures to reduce EMF.
- Consideration of the results for the next stage of investigation into the effects of EMF on electro-sensitive species.

Due to time limitations, it was agreed with COWRIE at the start-up meeting that CMACS would prioritise the modelling of EMF to a 132 kilo-volt (kV) Pirelli cable with an AC current of 350 amps in the marine environment and cable burial at a depth of 1m, as this was the most common cabling scenario. COWRIE also asked for consideration of EMF in brackish water environments, should further windfarm proposals consider routing power cables in estuaries.

2. REVIEW OF EXISTING INFORMATION

There is very little information available in the published literature or industry reports concerning either measured EMF generated by subsea power cables or actual investigation of the impact of EMF on species sensitive to these fields. This section of the report considers the available information that was gathered from published papers, reports and through consultation with a number of organisations and individuals (see Appendix I) and is broken down into two parts. Section 2.1 discusses UK offshore windfarm cabling strategies in the context of the first phase of developments in the UK. Section 2.2 describes the existing information regarding EMF generated by subsea cables and the work that has been carried out and/or planned for the future, in Europe.

2.1 UK OFFSHORE WINDFARM CABLING STRATEGIES

2.1.1 Factors affecting cabling strategies

The design of sub-sea cable systems for electricity produced by offshore windfarms will be influenced by several factors. Some of the factors are generic, while others are project-specific:

- Utility connection voltage – The vast majority of the current windfarm projects will be connected to regional distribution networks, rather than to the national transmission system. In England and Wales, these distribution networks currently cover 132kV and 33kV systems, as well as local 11kV distribution networks. Some of the phase 1 projects have secured connections at 33kV; others have secured connections at 132kV.
- Sub-sea cable technology – Three-core sub-sea cables using solid insulation (EPR or XLPE) are available for operation at voltages up to 132kV. Higher voltage cables that use oil as an insulating medium are not deemed to be environmentally acceptable owing to the potential risks associated with oil leakage. Cables with conductor sizes from 50mm^2 up to 630mm^2 are generally available, giving current carrying capacities up to approximately 700A. This equates to a power transmission capacity of up to 40MW for a single 33kV cable, or 160MW for a 132kV cable.
- Turbine electrical design – Most of the developers of the phase 1 windfarm projects are planning to use turbines rated at 2.75MW or more. These turbines are normally supplied with step-up transformers, with various options of HV voltage. These options typically include 20kV, 33kV and 36kV. Some HV switchgear is needed at the turbine, to protect the step-up transformer. This limits the HV voltage at the turbines to 36kV, as switchgear for higher voltage levels is either very large or very costly.
- Distance from shore – For large windfarm projects, the use of a single 132kV cable to shore can be a cost-effective alternative to the use of three or four 33kV cables. The installed cost (per kilometre) of a single 132kV cable is considerably lower than the installed cost of three 33kV

cables, but this solution requires an offshore substation in order to step up to 132kV from the windfarm collection voltage (usually 33kV). If the cable route to shore is short, the cost of the substation outweighs the saving on the cable. However, the offshore substation can often be justified if the cable route is much more than 10km. In addition, substations reduce the number of cables required and therefore the area affected.

2.1.2 Inter-turbine cables

The function of the inter-turbine cables is to collect the power from all of the turbines and bring it to one or more 'collection points' within the windfarm, from where it can be transmitted to shore. It is normal practice to cable several turbines together in a 'daisy chain', with each cable providing a link between two adjacent turbines. Each end of the cable is terminated onto the HV switchgear located within the turbine tower. A number of features associated with these cables are:

- Cable voltage – Because they connect to the HV switchgear at the turbines, the operating voltage for the inter-turbine cables is limited to 36kV. A nominal system voltage of 33kV is often planned for use in the UK, as this facilitates connection to the 33kV distribution system on-shore.
- Cable sizing – The sizing of the inter-turbine cables depends on the design approach used for the cable system. Some 'tree-like' designs involve the use of different cable sizes, with heavy cable being used for the main branches in the tree, and lighter cable being used for minor branches carrying the output from just one or two turbines. In 'looped' designs, the same cable size is often used for all of the inter-turbine cables.
- Cable armour – Single-wire armouring (SWA) is normally specified for inter-turbine cables. This level of armouring provides adequate protection against the kind of activities that are likely to occur within the wind turbine array (e.g. small boat anchors, marker buoy moorings etc). Double wire armoured (DWA) can be used but is heavy and inflexible cable such making it more difficult and expensive to produce and lay. The specific armouring required will however depend on the substratum type.
- Cable burial – Surface laying of the inter-turbine cables is normally deemed to be acceptable. Burial of the cables is sometimes specified if there are specific risks to exposed cables. Examples of such risks include sun damage to cables on sandbanks that are exposed at low tide, or cables becoming 'suspended' across deep troughs or ripples in the seabed. The type of substratum that the cable crosses will also determine whether cable burial is feasible (eg. sand versus rock).

2.1.3 Array-to-shore cables

The function of the array-to-shore cables is to transmit the power from the collection point (or points) within the windfarm to an appropriate cable connection facility at the shoreline. The electrical parameters of these cables will depend on the choice made between two options:

Option A: No voltage step-up offshore – The power produced by the windfarm is transmitted to shore at the collection system voltage. There is no need for an offshore substation. A few 'root turbines' act as the collection points within the windfarm. Each array-to-shore cable runs from a 'root turbine' to shore.

Option B: With voltage step-up offshore – The power produced by the windfarm is transmitted to shore at a different voltage level, greater than the collection voltage. An offshore substation is required, containing one or more step-up transformers. The offshore substation acts as the collection point within the windfarm. Each array-to-shore cable runs from the offshore substation to shore.

A third option, high voltage direct current (HVDC) is not economically viable at present due to the high cost of HVDC converters, however it may be used for sites situated further offshore in the future.

The design parameters of the array-to-shore cables can be discussed with reference to options A and B.

- Cable voltage – Given option A, the operating voltage for the array-to-shore cables is limited to 36kV because of the HV switchgear in the turbines. Under option B, the limiting factor is the availability of environmentally acceptable cable technology. At present, the limit is 132kV as cables rated to operate above 132kV require the use of oil insulation.
- Cable sizing – Given option A, the array-to-shore cables will normally be sized to minimise the number of cables required. This results in the use of very heavy cable (630mm^2 or greater). For option B, the size of the windfarm may not require the use of the heaviest cable. For example, a 100MW windfarm could be connected to shore using a single 300mm^2 cable rated at 132kV.
- Cable armour – Either single- (SWA) or double-wire armouring (DWA) may be specified for array-to-shore cables. Notwithstanding the costs and practical constraints of DWA, they tend to be used if the cable route crosses hard ground (ie. rock) and there is a risk of crush damage. Single-wire is often deemed to be adequate if the sea-bed is soft (sand or silt) and the cable is to be buried.
- Cable burial – Burial of array-to-shore cables is usually regarded as prudent, due to the risk posed by large vessels operating outside the windfarm boundary. Target depths of up to one metre are usually as depths greater than this are difficult to achieve in anything harder than sand or silt. Cable burial is costly, and this has to be weighed against the risks to the cable and the consequences of major damage.

2.2 CURRENT UNDERSTANDING OF THE EMF GENERATED BY SUBSEA POWER CABLES

A number of contacts (see Appendix I) provided information, via websites, email or documentation, for an assessment of current knowledge on the EMF generation of subsea power cables. The cables considered were mainly three-phase which have three separate cores/conductors, each of which is shielded by an 'earthed' insulation screen. This earthing effectively confines the E-field to within the cable and reduces the hazard of shock[2]. However, whilst it is possible to shield the E-field, the B-field cannot be effectively shielded in this way and as a result, there exists an electromagnetic field outside the cable and in the surrounding medium adjacent to the cable. During the assessment it became clear that opinions differed with respect to the magnitude of the B-field and its properties. Below is a summary of current understanding of EMF's generated by subsea power cables.

Pirelli provided information on EMF generated by the cables[3] that they manufacture. They stated that no electrical field is generated as the electrical field is confined to the metallic screen or shield of the insulation and that in most cases, this would be solidly bonded at both termination points.

Furthermore, Pirelli reported that 3-core cables are manufactured with metallic shields with the laid up bundle protected by armour wires. They stated that the close proximity of the core shields (i.e. touching in trefoil formation) and the overall armour, which is earthed at each end, would minimise the magnitude of the generated B-field. Their conclusion was that as the three cores are laid together in trefoil during manufacture and as the phase currents are balanced, the B-fields of the three conductors tends to be zero. As a result of this, the magnitude of the B-field in the proximity of the cable is regarded by Pirelli to be null and its presence in the sea bottom inert.

AEI Cables Ltd.[4] was able to calculate the reportedly small B-fields for a 33kV XLPE cable carrying AC currents of 359A and 641A. They give B-fields at 0m and 2.5m from a 33kV XLPE cable with a 359A current of 1.45 and 0.24μT respectively. When the current flow in the cable was increased to 641A, B-field strength at 0m and 2.5m increased to 1.7 and 0.61μT respectively. For reference, the Earth's geomagnetic field strength is approximately 50μT and thus, the reported B-fields at 2.5m from a cable, are less than $1/50^{th}$ of the Earth's geomagnetic field. However, it should also be noted that these small B-fields generated by power cables are 50Hz (UK mains power frequency) varying fields that marine organisms will perceive differently to the static geomagnetic field generated by the Earth. AEI stated that there was no E-field leaked by the cable as a result of cable shielding.

Dr. R. Bochert, Institut für Ostseeforschung Warnemünde,[5] Germany reported that cable technology is able to minimise E-fields by isolation. However, whilst there is no electrical field leakage, there is a

secondary electrical field induced by the B-field in the environment. The movement of water and marine organisms, such as a fish, through a B-field generates this 'induced' E-field. Dr. Bochert further reported that it is not possible to minimise the B-field and that neither sediment type nor salinity influences this B-field. (This finding holds true within 10m of the cable).

Eltra of Denmark modelled potential EMF generated by subsea power cables in relation to the Horns Rev offshore windfarm[6,7]. 33 and 150kV cables were modelled carrying 400 and 600A currents respectively. The modelling predicted that the 150kV cable carrying a current of 600A generated an induced electrical field of greater than 1000 μV/m to a distance of 4m from the cable. Additionally, the field extended for approximately 100m before dissipating. A 33kV cable carrying a current of 400A was predicted to generate a lower induced E-field of 1000 μV/m at the cable. The influence of the field was similar to the 150kV cable, extending some 100m, however, the strength of the field dissipated more quickly; at 4m from the cable, the E-field strength had reduced by more than 50%. Single-phase conductors were probably used; which would explain why the induced E-field observed for this model is relatively high.

From a biological perspective very little is known about the effects of EMFs associated with subsea power cables on organisms in the local environment[1]. Westerberg & Begout-Anras (1999)[8] investigated the orientation of silver eels (*Anguilla anguilla*) in a disturbed geomagnetic field created by the presence of a submarine high voltage direct current (HVDC) power cable. HVDC power cables pass a current in a single-conductor cable with the return current via the water. It should be noted that this type of cable is not characteristic of the AC cables currently proposed by UK offshore windfarms. In the Westerberg & Begout-Anras study, the B-field generated by the cable was of the same order of magnitude as the Earth's geomagnetic field at a distance of 10m. Of twenty-five female eels tracked, approximately 60% crossed the cable. Westerberg & Begout-Anras conclude that the cable did not act as a barrier to the eel's migration path in any major way, but concede that further investigation is required. In a more recent publication, Westerberg (2000)[9] reported similar results after investigating elver (a young stage in the eel life cycle) movement under laboratory conditions.

In 2001, an investigation of the effect of noise, vibration and electromagnetic fields on fisheries related species was carried out at the Vindeby wind farm, Denmark[10]. The aim of this investigation was to determine whether noise and vibration and/or EMF have affected fisheries species in the area of the windfarm and cable route. Poor weather conditions however, prevented survey work and so, the question at Vindeby remains unanswered. SEAS, Denmark intend to repeat this investigation at the Rødsand wind farm site. To date, baseline data have been collected on migratory and electro-sensitive fish species in the general area of the cable route. Monitoring of fish migration over the cable and any changes in electro-sensitive species number and abundance will be carried out between 2003 and

2005[11]. Similar investigations focusing on electro-sensitive fish species and their distributions along cable routes are planned at most offshore windfarms including several in the UK such as North Hoyle. For submarine cables, the influence of electromagnetic fields on marine organisms must be closely examined as EMFs outside the cables may have positive or negative implications for the organisms. Some literature shows that the sensitivity threshold of electrosensitive fish species could be much lower than the electromagnetic field level in close proximity to a cable[12]. Existing studies show that elasmobranchs can detect artificial bioelectric fields down to 0.5μV/m (=5nV/cm) and avoid fields of 1000μV/m (=10μV/cm) or greater[1]. Gill & Taylor[1] demonstrated that the dogfish, a species of elasmobranch, was sensitive to E-fields equivalent to those estimated to be emitted by power cables. Furthermore, the B-field generated by a subsea power cable may be of sufficient intensity to affect other species that have been shown to use geomagnetic fields generated by the Earth to orientate themselves in their environment. For example, cetaceans are thought to be sensitive to changes in the geomagnetic field of 30 ~ 60 nano-tesla (nT), and probably employ much finer levels of discrimination[13].

Therefore the current state of knowledge regarding the EMF emitted by undersea power cables is too variable and inconclusive to make an informed assessment of any possible environmental impact of EMF in the range of values likely to be detected by organisms sensitive to electric and magnetic fields. The remainder of the report sets out to determine the extent of the EMF, if any, by investigating both the electric and magnetic components of an EMF and considering the results in the context of EMF sensitive species.

3. MODELLING EMF

This section considers the modelling of electromagnetic fields generated by a 132kV XLPE three-phase submarine cable designed by Pirelli[14]. There are two components to the electromagnetic fields (EMFs) generated by such a cable, an Electric Field (E-field) and a Magnetic Field (B-field).

The E-field is produced because a voltage is applied to the cable. For a given set of cable properties the E-field is proportional to the applied voltage. Therefore, simulation results at 132kV may be scaled to different voltage levels through suitable scaling factors. For example, if the same cable was used at 33kV the simulation results for the E-field should be scaled by 0.25 (i.e. 33,000 / 132,000). As noted in section 2.2 modern, subsea cable design is expected to effectively contain the E-field within the cable if perfect shielding is assumed. Note, if the cable was not shielded the E-field would be expected to decrease with increasing distance from the cable.

The B-field is produced by current flowing through the cable. The magnitude of the B-field is proportional to the magnitude of the current for a given type of cable. Again the B-field scales with current (i.e. double the current and the B-field doubles). The strength of the B-field is also expected to reduce with increasing distance from the cable.

It should be noted that in AC cables the voltage and current alternate sinusoidally at a frequency of 50Hz. Therefore the E-field and B-field are also time varying and this time variation is expected to give rise to other voltages and currents being induced.

To ensure clarity, this section gives a description of the modelling software, cable geometry and common environment in which offshore windfarm cables are likely to be laid. The EMF generated is considered for cables with 'perfect' shielding and 'non-perfect' shielding.

3.1 INTRODUCTION TO THE SIMULATION SOFTWARE

For simulations of the EMF patterns of a device, geometrical modelling is necessary. The cross-section of a three-phase cable is uniform along the axis of the cable; therefore the field patterns in an entire cable can be modelled by simulating the fields in its cross-section (ie. 2-D). The 'Maxwell 2D' software program allows the simulation of electromagnetic and electrostatic fields in structures with uniform cross-sections[15] by solving Maxwell's equations using the finite-element method. The program divides the modelled structure into many smaller regions, which are represented as multiple triangles. The collection of triangles is referred to as the finite element mesh. The program computes

the electric and magnetic fields at the nodes (vertices) of triangles. The solved fields at each node are then represented as a separate polynomial and fields at points inside the triangles are interpolated from these nodal values.

Users of Maxwell 2D draw the structure and specify relevant material characteristics, boundary conditions describing field behaviours, sources of current or voltage, and the quantities required to compute. The simulator generates field solutions and computes the requested quantities. There are different field solvers for calculation of different alternating current (AC), direct current (DC) or static fields. Two field solvers (models) have been used in this project.

3.1.1 AC conduction field solver model

The AC conduction field solver model simulates and analyses conduction currents due to time-varying E-fields in conductors and lossy dielectrics. It can be used to model current distributions, E-field distributions and potential differences. In addition, any quantity that can be derived from the basic electromagnetic quantities can be analysed. The AC conduction field solver computes the electric potential, from which the E-field $\boldsymbol{E}(t)$, the electric flux density $\boldsymbol{D}(t)$ and the current density $\boldsymbol{J}(t)$ can be derived. Note, the "t" in brackets indicates that these quantities are time varying.

Maxwell's equations are the basic for computing electromagnetic field components[16]. The AC conduction field simulator solves for the electric potential in the following equation:

$$\nabla \cdot \left[s\,\boldsymbol{E} + jwe\nabla f \right] = 0 \qquad (1)$$

where f is the electric scalar potential, w is the angular frequency at which the potential is oscillating, s is the conductivity and e is the permittivity. All object interfaces are defined as natural boundaries, which simply mean that $\boldsymbol{E}$ and $\boldsymbol{J}$ are continuous across the object surface, according to the following relationships:

$$\boldsymbol{E}_{t1} = \boldsymbol{E}_{t2} \qquad (2)$$

$$\boldsymbol{J}_{n1} = \boldsymbol{J}_{n2} \qquad (3)$$

where $\boldsymbol{E}_t$ is the E-field strength tangential to the interface, and $\boldsymbol{J}_n$ is the conduction current density normal to the interface. 1 and 2 signify two different media types.

3.1.2 Eddy current field solver model

The eddy current field solver model simulates the effects of time-varying currents in parallel-conductor structures. It can be used to model eddy currents, skin effects and magnetic flux. In addition, any quantity that can be derived from the basic B-field quantities can be analysed. The eddy current field solver computes the magnetic vector potential, from which the B-field $\boldsymbol{H}(t)$, the magnetic flux density $\boldsymbol{B}(t)$ and the current density $\boldsymbol{J}(t)$ can be derived.

The eddy current field solver calculates the eddy currents by solving the magnetic and electric potentials in the following equation:

$$\nabla \times \frac{1}{m}(\nabla \times \boldsymbol{A}) = (s + jwe)(-jw\boldsymbol{A} - \nabla f) \tag{4}$$

where $\boldsymbol{A}$ is the magnetic vector potential and m is the permeability. All object interfaces are defined as natural boundaries, i.e., the tangential component of $\boldsymbol{H}$ and the normal component of $\boldsymbol{B}$ are continuous across the object surface, according to the following relationships:

$$\boldsymbol{H}_{t1} = \boldsymbol{H}_{t2} + \boldsymbol{J}_s \tag{5}$$

$$\boldsymbol{B}_{n1} = \boldsymbol{B}_{n2} \tag{6}$$

where $\boldsymbol{H}_t$ is the B-field strength tangential to the interface, $\boldsymbol{B}_n$ is the magnetic flux density normal to the interface, and $\boldsymbol{J}_s$ is the surface current density.

3.2 MODELLING OF THE CABLE

3.2.1 Geometrical modelling of the problem

Figure 3.1 shows the constructional geometry of the Pirelli 132kV XLPE submarine cable (ie. the cable components and positional relationships between them) given in its specification whilst Figure 3.2 shows the simplified geometry of the cable that was simulated in the Maxwell 2D software package. Dimensions of each section in the simulated cable model were identical to those of the real cable. The diameter of the cable is 18cm and consists of a triangular symmetrical arrangement of three single-core sub-cables, where the sub-cables are laid as at the corners of an equilateral triangle. Every core in the three-phase cable, comprising phases 1, 2 and 3 with 120° phase shift from each other, can be regarded as a return line of the two others. In each core, the lead sheath serves as a conducting screen to confine the E-field radial inside each sub-cable. Outer steel armouring provides stronger mechanical strength and added protection to the cable. Inside each core is filled with polyethylene XLPE, which has good electrical and thermal performance.

For the simulation of the submarine cable working in a real environment, we set up the simulation scenario where the submarine cable was buried in the seabed to a depth of 1 m beneath the seabed surface. Figure 3.3 shows the simulation scenario, with the cable laid perpendicular to the plane of the paper and its cross-section modelled as shown in Figure 3.2.

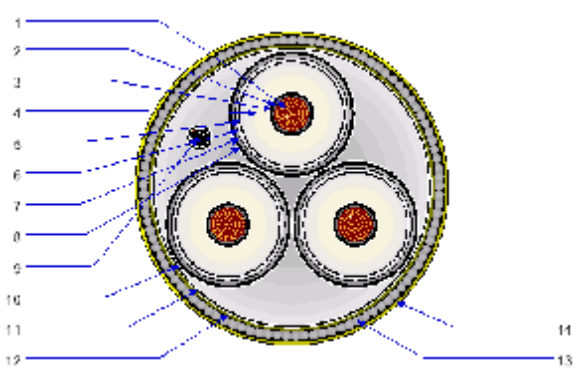

Item	Description	Details
1	Conductor	Copper
2	Water blocking	Water swellable compound
3	Conductor screen	Extruded semi-conductive
4	Insulation	XLPE
5	Core screen	Extruded semi-conductive
6	Water blocking	Tape
7	Lead sheath	Alloy C
8	Anti-corrosion	Polyethylene
9	Optional auxiliary cable	Optic fibre unit
10	Lay-up cores	
11	Binder	Tape
12	Armour bedding	Polypropylene string
13	Armour wires	Galvanised steel
14	Serving	Polypropylene string

Figure 3.1: Constructional geometry of the Pirelli 132kV XLPE submarine cable

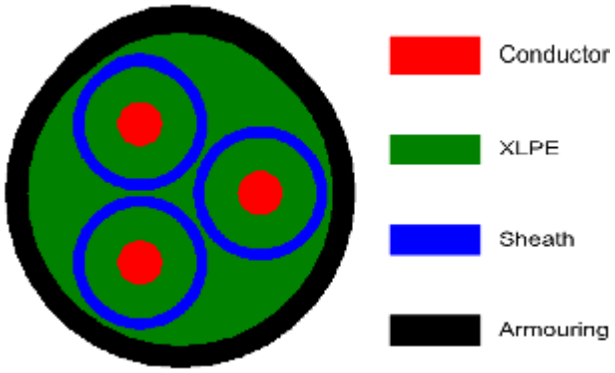

Figure 3.2: Geometrical model of the submarine cable for simulations

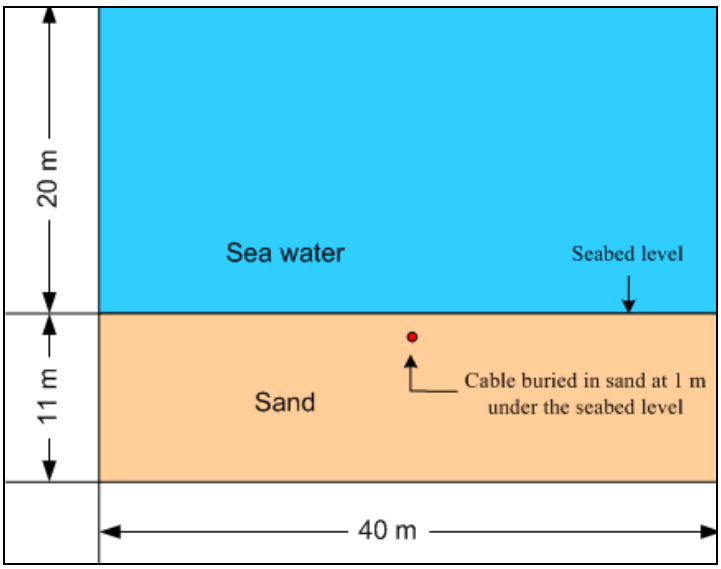

Figure 3.3: Cabling scenario of the submarine cable used in simulations (where m = metres)

3.2.2 Electromagnetic properties of the materials

To run the simulation, the electromagnetic properties of the materials used in the submarine cable model were defined (Table 3.1). All other materials of the cable are non-magnetic materials except the steel wire used for the armour, which has a relative permeability of 300. The permittivity e and permeability m of each material are given in terms of their relative values e_r and m_r respectively, and $e = e_r \cdot e_0$ and $m = m_r \cdot m_0$, where $e_0 = 10^{-9} / 36p$ F/m and $m_0 = 4p \times 10^{-7}$ H/m (Table 3.1).

Table 3.1 Electromagnetic properties of the materials of the submarine cable.

	Permittivity e_r	Conductivity s (s/m)	Permeability m_r
Conductor (Copper)	1.0	58, 000, 000	1.0
XLPE	2.5	0.0	1.0
Sheath (Lead)	1.0	5, 000, 000	1.0
Armour (Steel wire)	1.0	1,100, 000	300
Seawater	81	5.0	1.0
Sea sand	25	1.0	1.0

In the model the cable operated at 50 Hz (UK mains power frequency) with AC voltage of 132 kV between phases and AC current of 350A flowing in each conductor. With information on the geometry, electromagnetic properties of the cable and the excitation sources, the Maxwell 2D software computed the electromagnetic fields in the model.

3.3 SIMULATION RESULTS AND DISCUSSION

3.3.1 EMF generated by a cable with perfect shielding

3.3.1.1 AC Conduction field solver model

By assigning the time-varying voltage source to each conductor of the three-core cable, the E-field distributions were obtained using the AC Conduction Field Solver model. Figure 3.4 shows the simulated E-field strength inside all cores of the cable at different phases. Owing to the alternating voltage sources with a 120° phase shift at each core, the E-field inside each core alternately attains the maximum value (Figure 3.4). Metallic sheaths in the cable create earthed shields for all cores, so the E-fields are seento be strictly confined in each core (Figure 3.4) and have a radially symmetric distribution within the dielectric XLPE. Consequently, no E-field is leaked from each core, giving rise to no E-field outside the submarine cable, as shown in Figure 3.5.

The simulation results shown in Figures 3.4 and 3.5 are for ideal cases where the sheaths of the cable are 'perfectly' earthed.

Whilst the simulation shows that a perfectly shielded cable would effectively confine E-fields within each core, induced E-fields outside of the submarine cable may still be generated. Maxwell's equations tell us that alternating E-fields generate B-fields, which in turn generate induced E-fields. This is a result of the fact that AC currents flowing in each conductor of the cable generates changing B-fields around the conductor. This changing B-field 'induces' an E-field in the surrounding medium and eddy currents in the three conductors. These effects cannot be simulated with the AC Conduction Field Solver, but are considered in the next section.

Summary

The following points can be drawn in summary:

- Maxwell's AC Conduction Field Solver Model was used to investigate whether a 132kV XLPE submarine cable generates E-fields. This model assumed that the cable was perfectly shielded.
- The E-field results are scalable to other voltages. For example, the scaling factor for applying 33kV to the cable is 0.25 (i.e. 33,000/132,000).
- The model showed that the cable did not directly generate an E-field outside the cable.
- B-fields generated by the cable (modelled in Section 3.3.1.2), will however generate 'induced' E-fields outside the cable.
- This model could not quantify induced E-fields.

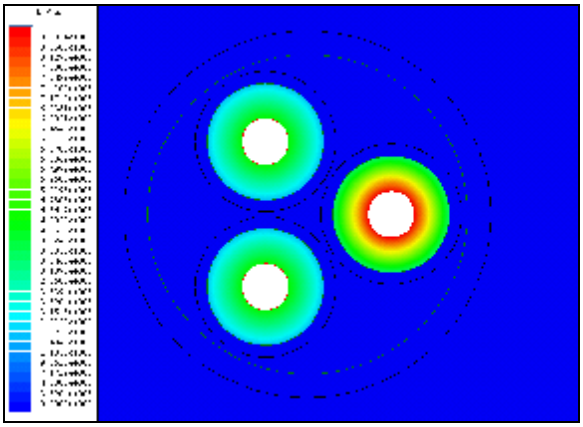

(a)

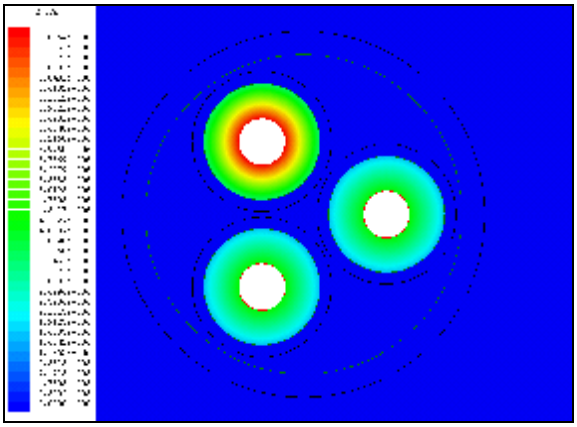

(b)

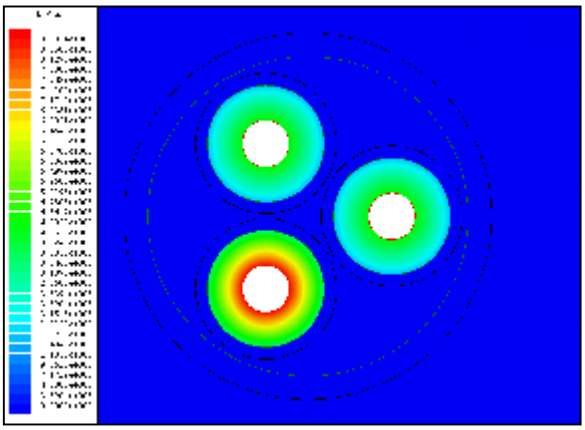

(c)

Figure 3.4: The electric field strength inside the cable at different phases: (a) $q = 0^{o}$; (b) $q = 120^{o}$; and (c) $q = 240^{o}$.

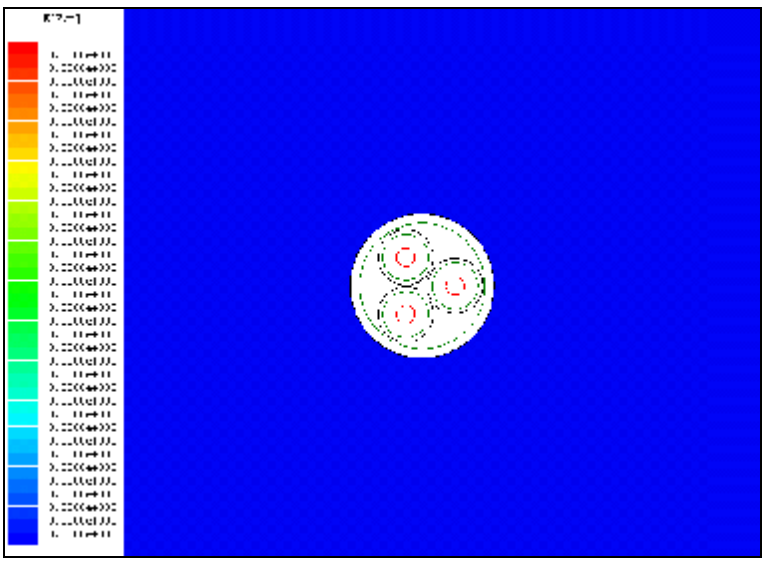

Figure 3.5: Magnitude of the electric field strength outside the cable (Geometrical dimension of the simulation: 1m ´ 1m)

3.3.1.2 Eddy current field solver model

An operational submarine cable will have alternating currents flowing in each conductor with a 120° phase shift at each core. This will generate changing B-fields around each conductor. Figure 3.6 shows the simulated B-fields inside the cable at different phases. It can be seen that the B-fields have a temporal rotation along the axis of the cable (Fig 3.6).

The sheaths of the cable can provide good shielding of the E-field, as discussed in Section 3.3.1.1 and shown in Figure 3.4, however, the sheaths cannot shield B-fields due to AC flowing in the cable. As a result of this, B-fields are expected to exist outside the cable.

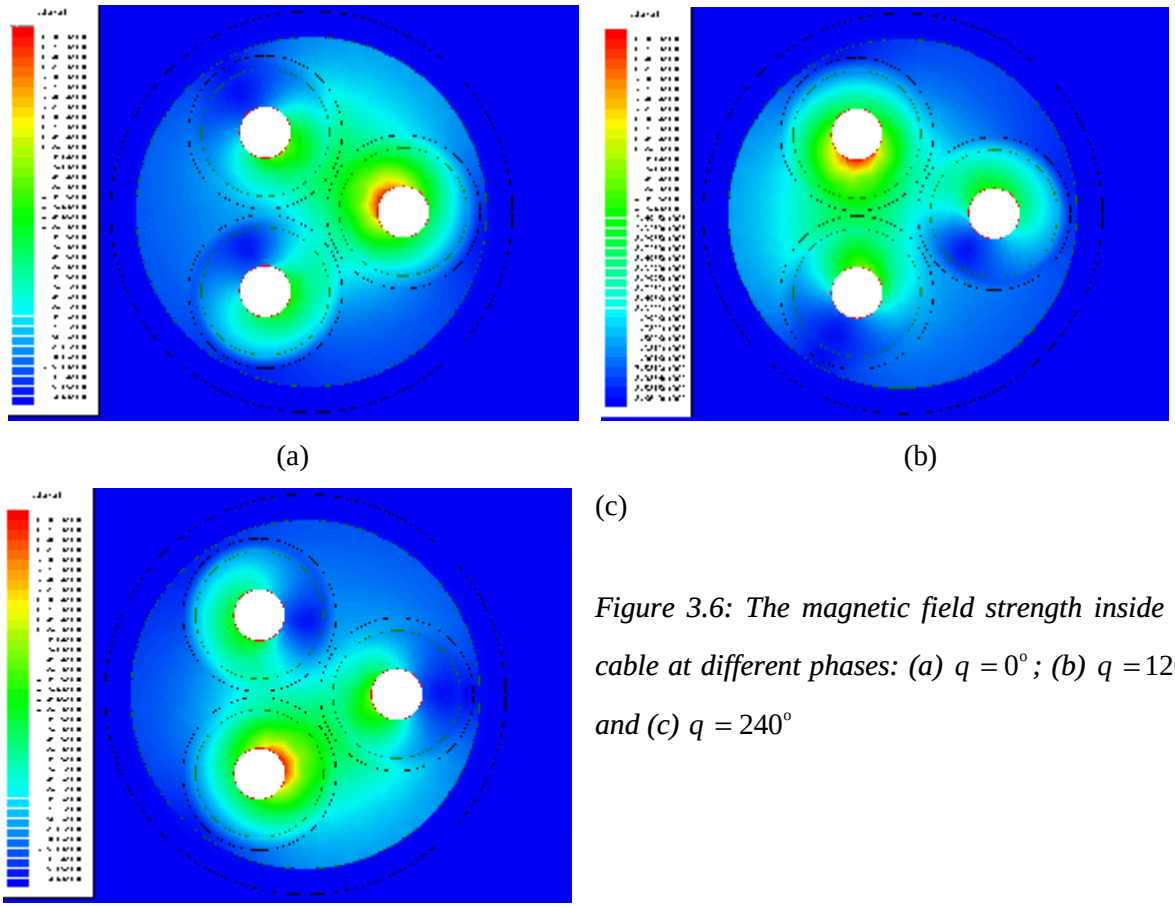

(a) (b)

(c)

Figure 3.6: The magnetic field strength inside the cable at different phases: (a) $q = 0^{o}$; (b) $q = 120^{o}$; and (c) $q = 240^{o}$

Figure 3.7 shows the simulated magnitude of magnetic flux density outside the cable with the cable buried 1m below the seabed. The dimensions of the problem simulated are given in Figure 3.3.

It is clearly seen that strong magnetic fields are present in close proximity to the cable and that these fields dissipate along the radial direction of the cross-section of the cable (Figure 3.7). It is worth noting that the B-fields at the same distance to the cable are identical, whether the observation point is in the seawater or in the sea sand. Continuous B-fields are present across the boundary between the

seawater and the sea sand as neither seawater or sea sand have magnetic properties i.e. the sediment type in which a cable is buried has no effect on the magnitude of B-field generated.

The magnitude of the B-field on the 'skin' of the cable (i.e. within millimetres) is approximately 1.6μT. As a result of using 50Hz AC, this B-field will vary predictably with time and will be superimposed onto any existing B-field (eg. the Earth's geomagnetic field which has a strength of approximately 50μT). The strength of the B-field associated with the cable diminishes rapidly and in a non-linear manner with distance and background levels are reached within 20m (Figure 3.7). The maximum B-field strength of 1.6μT corresponds well with the B-field strength calculated by AEI Cables Ltd[4] of 1.45μT for a power cable carrying a similar current.

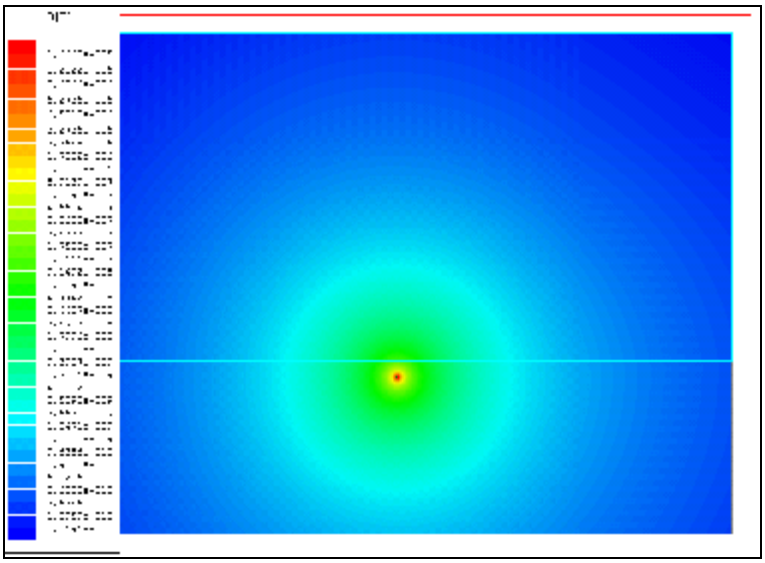

Figure 3.7: Magnitude of the magnetic flux density outside the cable
(Geometrical dimension of the simulation is as given in Figure 3.3)

Figure 3.8 shows the vector view of the magnetic flux density outside the cable at different phases. In contrast to the case of a cable with a single-core, the B-fields around the three-phase cable are no longer concentric to the axis of the cable and are not uniformly circular. This is a result of a specific phase of the current flowing in each conductor is different from that in the two others.

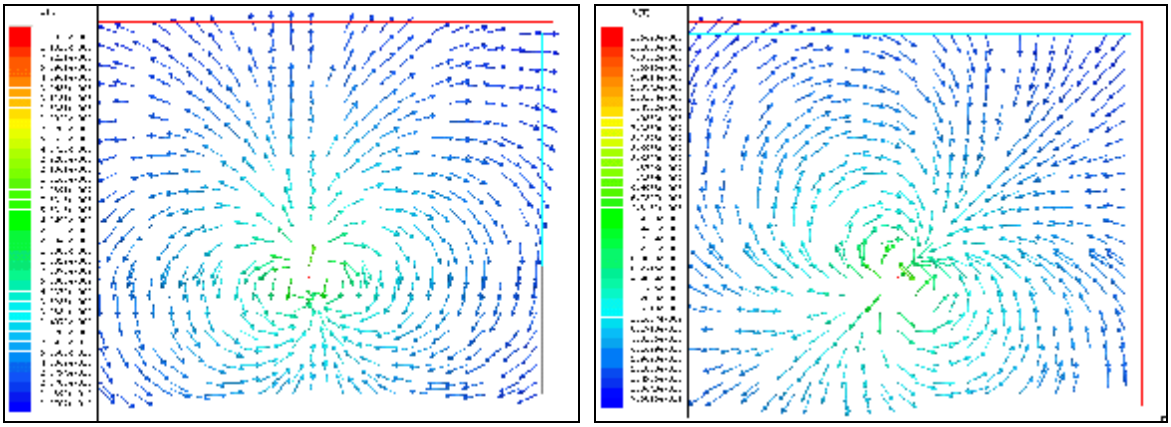

(a) (b)

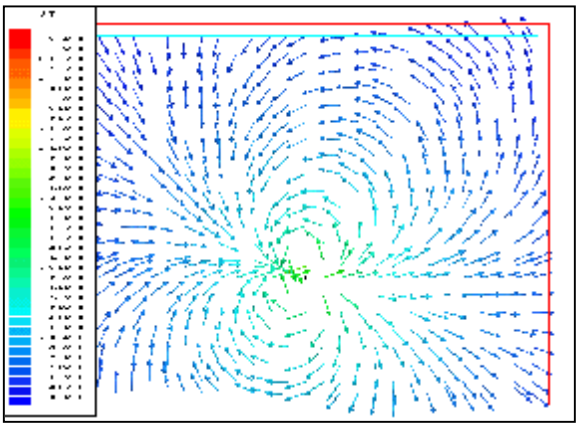

(c)

Figure 3.8: The vector magnetic flux density outside the cable at different phases: (a) $q = 0^{o}$; (b) $q = 120^{o}$; and (c) $q = 240^{o}$.

The time-varying currents flowing in the cable produce time-varying B-fields outside the cable in the plane perpendicular to the conductors in which the currents flow. In turn, these B-fields 'induce' E-fields around the cable. The eddy current field solver of the Maxwell 2D programme computes the current density $\boldsymbol{J}(t)$, rather than the E-field strength $\boldsymbol{E}(t)$. According to Maxwell's theorem, the link between the B-field strength, the current density and the E-field strength in a medium is described as follows

$$\nabla \times \boldsymbol{H} = \boldsymbol{J}_e + \boldsymbol{J}_d \qquad (7)$$

where $\boldsymbol{J}_e$ is the induced eddy current density due to the time-varying B-fields, and $\boldsymbol{J}_d$ is the displacement current density due to the time-varying E-fields. The resultant complex total current density $\boldsymbol{J}$ is therefore related to the E-field strength as:

$$\boldsymbol{J} = s\boldsymbol{E} + jwe\boldsymbol{E} \qquad (8)$$

Figure 3.9 shows the simulated current density in both the seawater and the sea sand. Since the seawater and the sea sand have different electrical properties (see Table 3.1) with different conductivity values, the simulated current density is discontinuous across the boundary between the seawater and the sea sand. Due to the higher conductivity and permittivity of seawater, the current density at an observation point in the seawater is higher than that in the sea sand, both at the same distance to the cable.

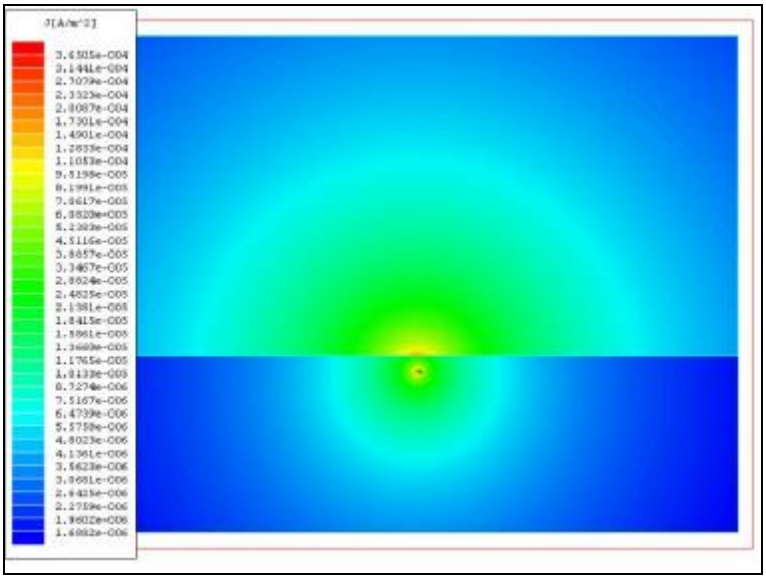

Figure 3.9: Magnitude of the current density outside the cable
(Geometrical dimension of the simulation is as given in Figure 3.3)

The magnitude of the current density on the 'skin' of the cable (i.e. within millimetres) and on the seabed directly above the cable is 0.000365A/m^2. Using Equation (8), this can be approximated to E-field strength of 91.25μV/m (assuming a seawater conductivity of 4 Siemens per metre [S/m] ie. fully marine). The E-field in the seabed dissipates rapidly to only 1 or 2 μV/m within a distance of approximately 8m from the cable. At the same distance in the seawater however, the E-field strength is approximately 10μV/m (=0.1 μV/cm).

Hence, the induced current densities are effectively the same on the "skin" of the cable and on the seabed, therefore the mitigation effects of burying the cable one metre into the seabed are negligible from an electromagnetic view. The induced current density in the seawater decreases with distance from the cable and there is a more rapid reduction within the sediment (see Figure 3.9). The linkage between the induced current and E-field is defined by Equation (8).

Gill and Taylor[1] determined through a literature review and experimentation that dogfish were attracted to E-fields ranging from 0.5μV/m - 10μV/m, whereas they avoided fields of 1000μV/m.

Therefore, a dogfish (or another species with similar sensitivity) may be able to detect a buried cable within a number of metres of the cable (horizontally along the seabed or vertically in the water column).

The simulation has been conducted using a three-phase cable, characteristic of UK windfarm cabling proposals, and is different from a single-core cable modelled at Horns Rev. As such, direct comparison of the results presented above with the results of modelling for Horns Rev is not possible at this stage.

Summary

The following points can be made in summary:

- Maxwell's Eddy Current Field Solver model was used to investigate B-field generated by a 132kV XLPE submarine cable. This model assumed that the cable was perfectly shielded.
- The results of the simulation showed that B-fields are present in close proximity to the cable and that any non-magnetic sediment type in which a cable is buried has no effect on the magnitude of B-field generated.
- The magnitude of the B-field on the 'skin' of the cable (i.e. within millimetres) is approximately 1.6μT which will be superimposed on any other B-fields (eg. earth's geomagnetic field).
- The magnitude of the B-field associated with the cable falls to background levels within 20m.
- An induced E-field is generated by the B-field, irrespective of shielding.
- The induced E-field in the seawater decreases with distance from the cable and there is a more rapid reduction within the sediment
- The strength of the induced E-field is within the sensitivity range of dogfish.

3.3.2 EMF generated by cables with non-perfect shielding

In section 3.3.1, it is shown that the E-field would be strictly confined within each core of the cable due to the perfect shielding of the conductor screen, i.e., the sheath of each core is well earthed and the potential of the sheath is zero.

In this section, the model simulates the situation where the conductor-shielding screen is not well earthed and thus, the potential of the cable sheath is not zero. A reference circular boundary with zero potential at 10m away from the axis of the cable was defined. Seawater was modelled as the medium between the cable and the reference boundary. Due to the precision limitation of the software, Maxwell 2D's AC conduction field solver model could only simulate the model with the conductivity of the sheath of up to 3000 S/m.

Figure 3.10 describes the simulated E-field strength between the cable and the reference boundary, with the conductivity of the sheath and armour set at 1000 S/m. The E-field is radially distributed around the cable and attenuated with distance (Figure 3.10). The simulation was run a second and third time with the conductivity of the sheath and armour set at 2000 and 3000 S/m.

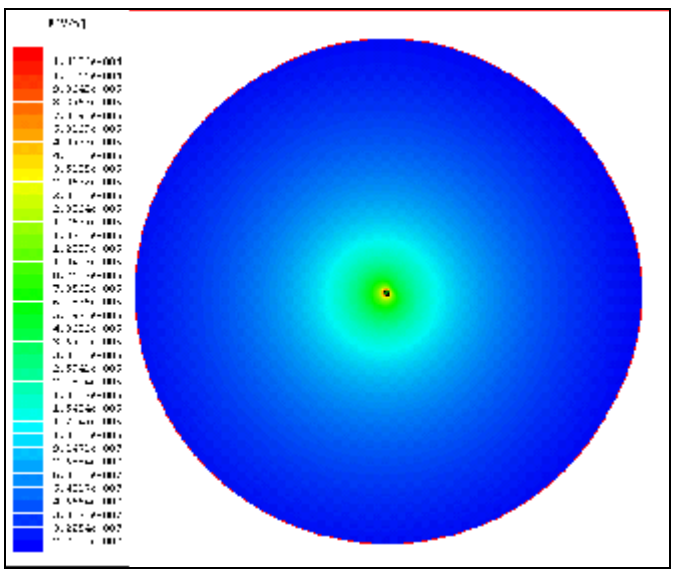

Figure 3.10: The electric field strength within the seawater medium.

The simulated E-field strength with distance from the cable is shown in Figure 3.11. Again it can be seen that the E-field strength outside the cable monotonically decreases with the conductivity of the sheath and armouring materials used for the cable. Therefore, it is expected that even though the

sheath and armour are not well earthed, the E-field strength at or above 1m distance from the cable is very small for high conductive sheath and armouring materials.

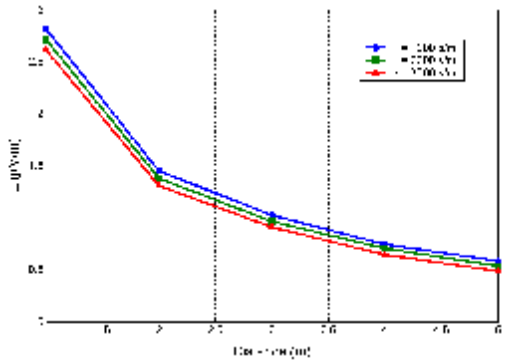

Figure 3.11: The electric field strength outside the cable for different conductivity values

Summary

The following points can be made in summary:

- An E-field would be generated outside a cable owing to non-perfect shielding/earth.
- This additional E-field is smaller than the normal induced E-field and decreases with the distance from the cable. It is not considered additive to any existing E-field.
- Burying the cable one metre deep would reduce the emitted E-field at the seabed.

3.4 CONCLUSIONS FROM MODELLING EMF WITH AND WITHOUT PERFECT CABLE SHIELDING

The Maxwell 2D programme was used to investigate EMF generated by 132kV XLPE three-phase submarine cable with an AC current of 350A through the application of two models; the AC Conduction Field Solver and the Eddie Current Field Solver.

The results of simulations showed that a cable with perfect shielding i.e. where conductor sheathes are grounded, does not generate an E-field directly. However, a B-field is generated in the local environment by the alternating current in the cable. This in turn, generates an induced E-field close to the cable within the range detectable by electro-sensitive fish species. The induced E-field is related to the current in the cable. A smaller current would proportionally produce a lower induced E-field, i.e. a cable current of 175A will give rise to half the induced current density at 350A and therefore half the induced E-field.

Simulations of a 132kV XLPE three-phase submarine cable with non-perfect shielding, i.e. where there is poor grounding of sheathes showed that there is a leakage E-field (not induced), but it is smaller than the induced E-fields. Again if the cable were operated at a lower voltage the electrical field results would need to be scaled. e.g. for a 33kV cable the scaling factor is 0.25.

4. MEASURING EMF IN THE ENVIRONMENT

4.1 INTRODUCTION

To directly measure the electromagnetic emission from undersea cables two sensors were developed, one able to detect B-fields and the other E-fields when placed near to a three-phase AC power cable in seawater. These sensors are briefly described in this section and circuits included in Appendix II.

The sensors were tested and calibrated in the laboratory, first at the bench and then in a seawater tank. *In situ* site trials were then undertaken at Rhyl in the Clwyd Estuary.

4.2 DESIGNING THE MAGNETIC AND ELECTRIC FIELD SENSORS

4.2.1 The Magnetic field sensor

Hall effect and the Fluxgate sensors are commonly used to measure magnetic fields of around 100 μT and 14 nT respectively. They are capable of measuring fields over a wide range of frequencies from 0 Hz (DC) to several 1000 Hz. Both are able to measure non-varying signals which means that they are used to detect the earth's B-field (≈50 μT), or the field from high voltage direct current links (HVDC)

Since the primary interest was in the mains power frequency (50 Hz) an alternative design based on a search coil was used. In a search coil varying B-fields produce a voltage that is proportional to the B-field. A differential electronic amplifier provided gain thereby increasing the B-field sensitivity of the sensor, while also reducing its sensitivity to E-fields.

The system was calibrated using a 70 nT $_{RMS}$ field generated from a 600 mm diameter coil. Experiments performed on site indicated that the unit had a minimum sensitivity of 0.5 nT $_{RMS}$.

The sensor proved reliable but needed to be held stationary to prevent pick-up from the earth's B-field, which can interfere with readings. This pick-up could be reduced and the sensitivity increased further by the addition of a band-pass filter.

4.2.2 The Electric field sensor

Detecting very low electric fields within the range that electro-receptive fish are sensitive to required a sensing system able to detect fields of around 1 to 10 μV/m. Two E-field sensors were developed:

- A high input impedance electric field sensor
- A low input impedance electric field sensor

4.2.2.1. The High input impedance electric field sensor

Electrodes in contact with water generate a relatively large electrode voltage of approximately 200 mV. This varies by a few 1000 μV with the salinity and also with temperature (approximately 1000 μV/˚C). Electrode voltage variations that occur at the mains power frequency may be perceived as being due to effects from the mains power-line. In order to prevent this an E-field sensor with a high input impedance was developed.

To separate the electrode from the seawater a 1-mm thick epoxy layer was used which acted as a capacitor coupling the signals from the seawater to the 4-cm² electrode without producing an electrode voltage. The epoxy layer used had a capacitance of approximately 12 pF which was smaller than that of other sensors that have been developed. One problem that resulted was this produced a large amplifier input current noise which limited the sensitivity of the sensor system. Therefore, the resulting noise limited the minimum detectable E-field from a 100 mm long sensor to 155 μV/m. Furthermore, the sensor was sensitive to vibration and also needed time to recover following exposure to voltages exceeding a few millivolts.

4.2.2.2. The Low input impedance electric field sensor

A low impedance sensor was then developed that works in a similar way to a fish ampullary electro-receptor system.

The low impedance E-field sensor used 3 cm² lead electrodes 10-cm apart. Lead has a very low electrode-to-electrode voltage and so minimised any electrode noise. The electrodes were polarisable meaning they did not react chemically with the water, instead charge would have built up on the surface of these electrodes, thereby acting like a capacitor (with a capacitance of around 100 μF per cm²). The DC current flowing through the electrodes had to be low (around 1 μA), hence low leakage capacitors were used to connect the electrodes to the rest of the circuit.

The sensor head (Figure 4.1), was made symmetrical to minimise the cross-sensitivity to B-fields when immersed in water. The head (enclosed in thin foil) and sensor electronics were tested and found to have a negligible B-field sensitivity (less than 10 μV/m in a 5000 nT field).

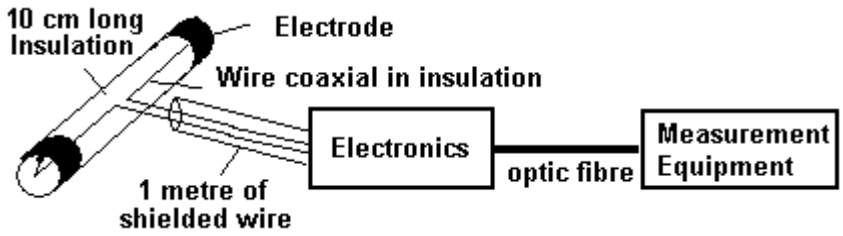

Figure 4.1: Low input impedance electric field sensor system

The sensor head was connected to the electronics by a short-shielded lead (Figure 4.1). The sensor electronics amplified the voltage before it was transmitted to the measurement equipment using a fibre optic cable. This arrangement ensured that the B-fields and ground loops did not interfere with the measurement process. The electronics of the systems would only sense signals as low as 0.42 μV_{RMS} at 50 Hz. This gave the 100 mm long sensor a minimum detectable E-field of 4.2 $\mu V/m_{RMS}$.

To calibrate the sensor it was placed in an aluminium enclosure then connected to a signal generator via a 100 dB attenuator.

4.3 LABORATORY TESTING

Prior to site trials at Rhyl a number or experiments were performed in a 46 cm wide x 26 cm deep x 90 cm long tank.

Initially the tank was filled with tap water (with a conductivity of 0.17 milli-siemens/cm) and a standard household 3-core mains electricity cable (with no screen or armour) placed in it. With the cable connected to a 120 V_{RMS} voltage, and with no current flowing, the high-impedance E-field sensor was able to detect a field of 2200 $\mu V/m_{RMS}$ close to the cable but was unable to detect low E-fields of a few hundred $\mu V/m_{RMS}$.

The low impedance sensor was then tested in the water filled tank with added sea salt to a concentration of 33 g/Litre (conductivity 45 milli-siemens/cm). With the cable connected a 240 V_{RMS} voltage, and with no current flowing, the E-field 100 mm from the cable was 25 $\mu V/m_{RMS}$.

A mock cable was then constructed to mimic some of the characteristics of an undersea power-line. Its cross-section is shown in Figure 4.2.

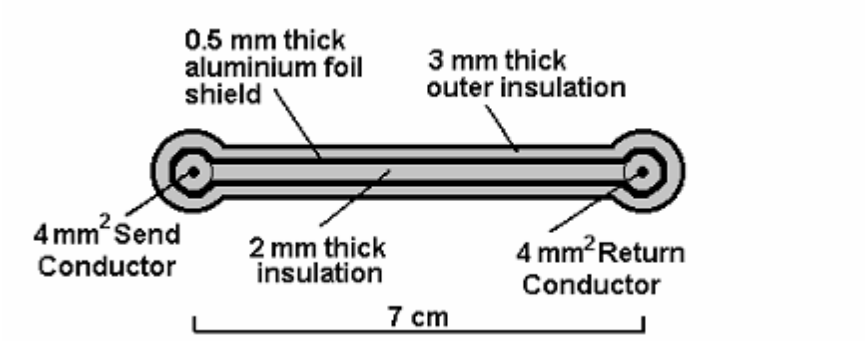

Figure 4.2 Cross section of the mock cable

The mock cable was connected to a 240 V_{RMS} voltage with no current flowing and the E-field was measured parallel to the conductor in the surrounding seawater at three set distances (Figure 4.3). These levels were probably higher than would occur with a real cable as the thin foil shield used would not be as effective at reducing E-field emission as the sheath and armour on a real cable. However this higher than expect field could be compensated by the lower voltage used for the test (200 V_{RMS} rather than 11/33 kV_{RMS}).

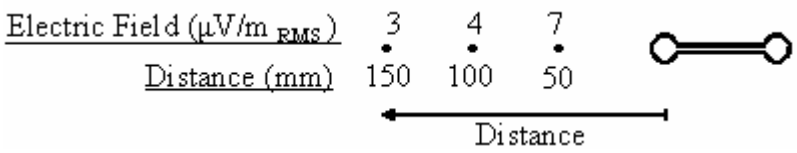

Figure 4.3 Electric field near the mock cable carrying a voltage

The connections were altered to carry a 50 Hz current of just 0.5 A_{RMS}; this was approximately 0.2% of the current likely to be carried by a real cable. The voltage difference between the send and the return ends of the conductors was negligible (0.5 V_{RMS}). The B-field measured around the mock cable was large (shown in Figure 4.4). The B-field was higher than would occur with a real cable carrying 0.5 A_{RMS} since the mock cable had no outer armour to reduce B-field emission, however a real cable would carry a far higher current.

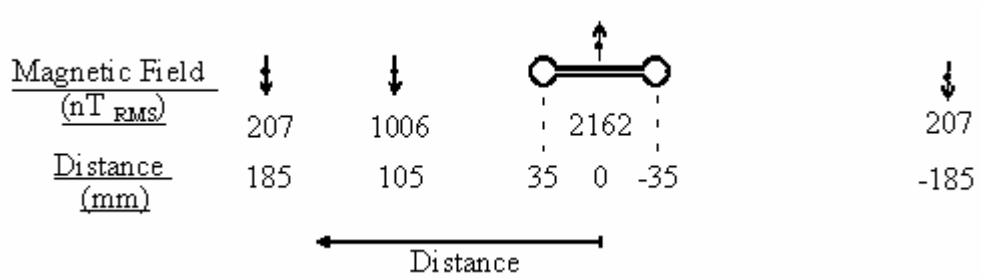

Figure 4.4 Magnetic field near the mock cable carrying a current

The low-impedance E-field sensor was then used to detect the E-field that was induced in the seawater tank by the time varying B-field produced by electric current flowing in the cable. The induced E-field measured is shown in Figure 4.5.

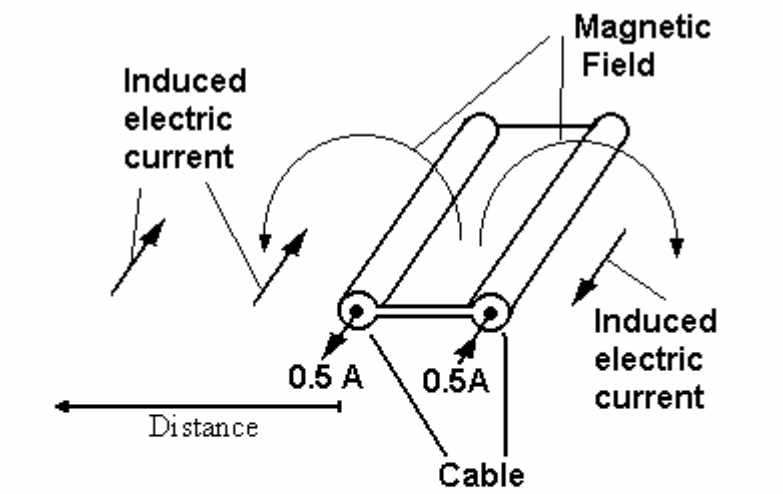

Induced electric field (μV/m) (measured)	11.7	20
Distance (mm)	100	50
Induced current density (μA/m²) (calculated)	47	82

Figure 4.5 Induced electric field the near mock cable carrying a current

Unlike the high impedance E-field sensor, the low impedance sensor recovered immediately from exposure to large E-fields.

The laboratory measurements of electric and B-fields agreed with the values expected from calculations.

4.4 FIELD TESTING

4.4.1 Introduction

Site trials were undertaken to test the magnetic and E-field sensors and evaluate the levels of magnetic and E-field emission from a real cable *in situ*. The aim of this investigation was to determine the following:

- Whether the sensors built could measure and detect electric and magnetic fields in a marine environment, and
- How these fields compared with the predictions of the modelling (Section 3).

Measurements were taken in the vicinity of power cables crossing the Clwyd Estuary at Rhyl, North Wales. This site was selected for the following reasons:

- The presence of a 33kV and an 11kV underwater cables
- Proximity to Liverpool if repeat measurements were required due to complications
- Site access and personal knowledge of the environment.

Figure 4.6 shows the location of the two cables running across the estuary upstream of the nearby Foryd Bridge (A494). Both cables lie approximately 1m below the surface of marine muddy sand.

The 33 kV three-phase cable carried $50A_{RMS}$ per phase. The cable has a metalised foil sheath surrounding each conductor. An outer lead sheath enclosed all three phases separated from the foil screens by paper insulation and the armour was provided as steel wire. The cable conforms to the British Standard BS-6480.

The 11 kV three-phase cable carried 60 A_{RMS} per phase. Each of the three phases was sheathed. An outer corrugated aluminium sheath enclosed all three phases and the cable conforms to the Electricity Association Technical Specification EATS 09-12.

4.4.2 Methodology

The electric and magnetic fields were measured with the sensors at the following radial distances upstream from each cable: 0m (i.e. directly above the cable), 1m, 2m, 5m, 10m, 20m and 400m. Note: the low impedance E-field sensor was adjusted to cover the range 6 to 100 $\mu V/m_{RMS}$.

The average of the sensor readings taken over a 10 second interval was recorded with the sensors submerged to a depth of approximately 1.5m below the surface of the water on an incoming tide.

The salinity of the estuary at the start of the test was approximately 10% seawater, with an electrical conductivity varying between 1.7 to 3 milli-siemens/cm depending upon location.

Electric and magnetic fields are directional (vectors) so readings were taken in both the vertical axis and horizontal axis (perpendicular to the cable) these readings were then combined together to give the magnitude of the field.

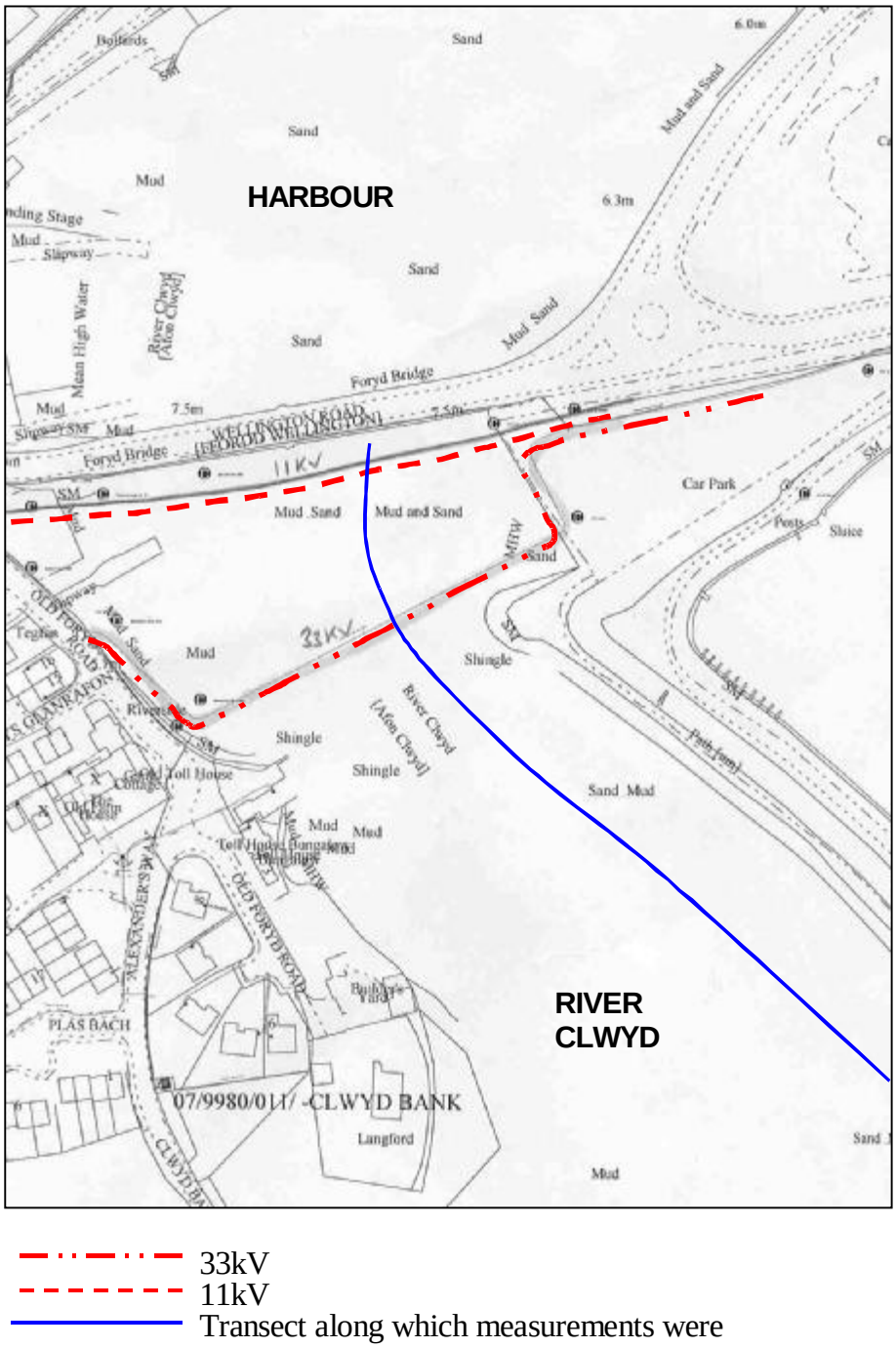

Figure 4.6: Location of 33 kV and 11 kV power cables at Rhyl and transects along which measurements were taken.

4.5 RESULTS

4.5.1 Magnetic field sensor

Near the 33 kV cable the magnetic field was measured as 50 nT $_{RMS}$ orientated 56˚ from vertical. The field decreased with distance from the cable axis (Figure 4.7). The orientation of the field beyond 5m was approximately 0˚ from vertical and at 400 metres from the cable the sensor picked up only noise (0.5 nT $_{RMS}$)

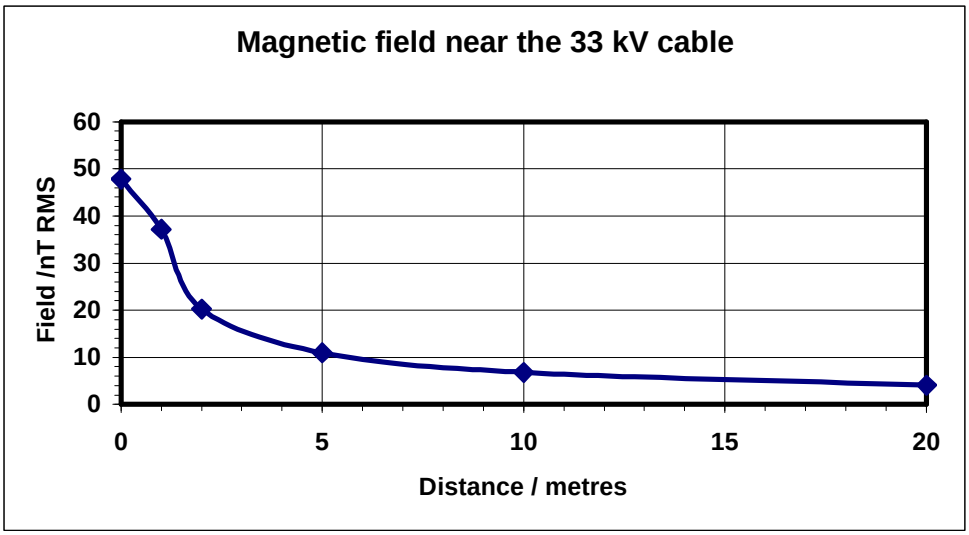

Figure 4.7 Magnetic field near the 33 kV cable

The position of the 11 kV cable was not precisely known, due to lack of markers, however it was located using the B-field sensor. Figure 4.8 shows the measured B-field; the negative distance readings were limited by the A494 Bridge and movement further than 15m in the positive direction would have led to interference from the 33 kV cable. The field from the 11 kV cable appeared to be more widely distributed than the 33 kV cable which may have been a consequence of the individually sheathed conductors.

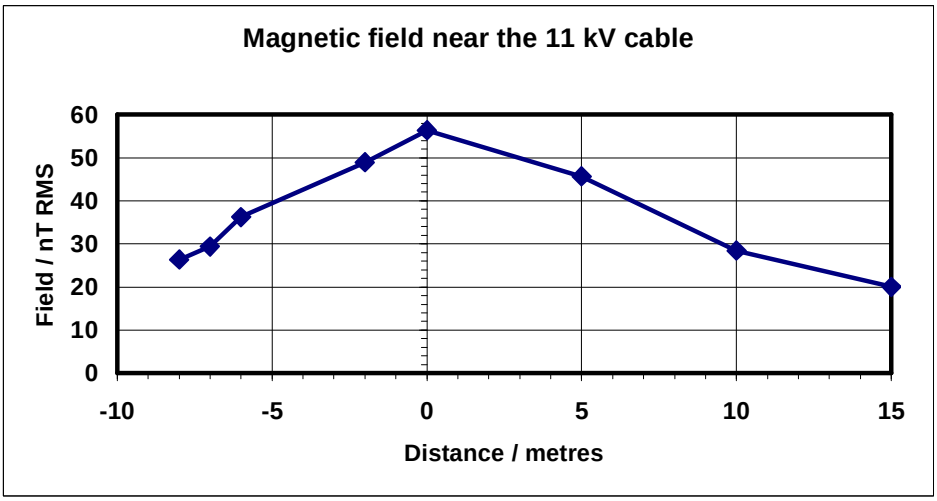

Figure 4.8 Magnetic field near the 11 kV cable

4.5.2 Electric field sensor

The low impedance electric field sensor produced a maximum output when placed in the estuary (indicating an E-field in excess of 70µV/m). The output did not change with orientation. The sensor continued to produce the same maximum output when positioned and immersed in the seawater 400 and 1000 metres from the power cable.

Calibration tests were performed before and after the site trials (Figure 4.9). The tests indicated the sensor was operational throughout the site trials, and that the E-field measurement was genuine.

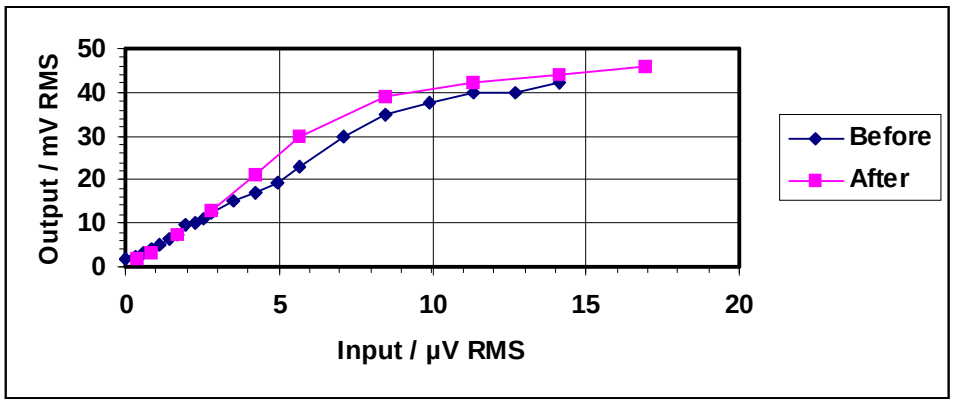

Figure 4.9 Calibration tests before and after site trials

Subsequent enquiries to the power company owning the cables revealed that whilst the 33kV cable conforms to the BS-6480, it is actually missing the steel wire armour, and is thus, un-armoured.

This lack of armouring would contribute to, but does not explain, the large E-field detected in the vicinity of the cable. Measurements taken at a distance of approximately 1 kilometre along the coast still recorded an E-field of greater than 70µV/m. It is not known whether the 3 phase currents were balanced. A larger current in one phase would have produced a larger than expected B-field and ultimately a larger induced E-field. Tidal movement will also have had an effect but this was not been quantified. Time limitations prevented further investigation of the measured E-field or further measurements carried out at an alternative site.

4.6 METHODOLOGY FOR CALCULATION OF EMF

A method is given below for calculating the induced E-field around a low frequency (such as 50 Hz) AC power cable due to the emanating B-field. This method does not consider E-fields generated as a result of non-perfect shielding or induced E-fields generated by movement of water through the B-field generated. Furthermore, this method requires *in situ* measurement of the B-field generated by an operational cable.

A number of factors can influence the measured B-field; therefore the field should be measured at various distances using apparatus such as that developed and reported in section 4, or by using a commercial magnetometer with sufficient sensitivity. Tests need to be performed several hundred metres from other cables or electrical equipment and care taken to ensure the B-field recorded is not emanating from the current supply apparatus or load at either end of the cable. The magnetometer should be orientated to give a maximum reading. Furthermore, measurements should be taken with the magnetometer at a depth of 0.5 to 1m of seawater directly over the cable.

The B-field measurable near a power-line (carrying an electric current) can be approximately related to an induced E-field in the surrounding medium (eg. the seawater) by the following equations:

	Electric Field (V/m) ≈ 2 * π * Power frequency (Hz) * Magnetic Flex Density (T)
Or	
	Electric Field (μV/m) ≈ 2,000 * π * Power frequency (Hz) * Magnetic Flex Density (nT)
Where	
	The power frequency used in the UK is 50 Hz.

This can also be related to the electric current density in water using the equation:

	Current Density (A/m²) = Electric Field (V/m) * Conductivity (S/m)
Or	
	Current Density (A/m²) = Electric Field (μV/m) * Conductivity (mS/cm)/10,000,000
Where:	
	Conductivity of Freshwater ≈ 0.025 Siemens/m (S/m) = 0.25 milli-Siemens/cm (mS/cm)
	Conductivity of Sea water ≈ 4 Siemens/m (S/m) = 40 milli-Siemens/cm (mS/cm)

4.7 CONCLUSIONS DRAWN FROM MEASURING EMF

The following points can be drawn in conclusions:

- Both magnetic and electric fields were detected.
- The B-field sensor developed performed well in the laboratory and site trials. It was able to detect B-fields down to 0.5 nT $_{RMS}$.
- The B-field level measured during site trials (56 nT $_{RMS}$) closely matched levels predicted by modelling (Section 3). This validates the model used for B-field calculations.
- Tests in the seawater tank in the laboratory showed that the E-field measured does not vary significantly with the shape of the sensor. This result implies the E-field in the water can be calculated from the current density using the following equation:

$$\text{Electric field } (\mu V/m) = \frac{1000000 \bullet \text{Current density } (A/m^2)}{\text{Conductivity (siemens/m)}}$$

$$= \frac{10000 \bullet \text{Current density } (mA/m^2)}{\text{Conductivity (milli-siemens/cm)}}$$

(For seawater the salinity/conductivity is approximately 4 S/m or 40 mS/cm)

- The modelling (Section 3) predicted that the B-field observed during field trials would induce an electric current density in the seawater of 0.1 mA/m² with a cable buried to a depth of 1m. It therefore follows from the above conclusion that the induced E-field in the water would be around 25 μV/m.
- Tests performed on a mock power cable indicated that with no armour or shield the B-field outside the cable is very high at approximately 1000 μT $_{RMS}$. This is a similar level to that predicted for single-phase power cables[12].
- A low input impedance E-field sensor was developed that had sensitivity comparable to that of electro-sensitive fish. During site trials this sensor detected a large E-field (above 70 μV/m) sufficient to overdrive the sensor.
- A contributory factor to this field may have been the lack of steel armour in the 33kV cable at Rhyl. However, this fact does not completely account for the large E-field detected at a distance of approximately 1 kilometre from the cable. Time limitations did not allow further investigation of the detected field.

- High input impedance E-field sensors tend to be sensitive to sound; therefore producing a sensor with sufficient sensitivity for this application (i.e. low output noise) would be difficult and would require further work.

5. MITIGATION FOR EMF

This section considers mitigation for EMF generated by the present industry standard sub-sea power cables. Three areas are considered:

- Effects of permeability of the power cable armour
- Effects of conductivity of the cable sheath and armour
- Effects of cable burial to a depth of 1m below the seabed

5.1 EFFECTS OF PERMEABILITY OF THE CABLE ARMOUR

In the manufacturing process of the submarine cable, armouring is usually provided in the form of steel wires or tapes around the cable[2]. The purpose of armouring is to enhance the mechanical strength of the cable. In the simulations carried out in Section 3, steel wires were assumed as the material for armouring. However, steel tape can also be used as an armouring material, but its permeability is very different from that of a steel wire. The relative permeability of steel wire is about 300, but that of a steel tape is about 3000[2]. The strength of B-fields produced by the cable are dependent not only on the amplitude of current sources, but also on the electromagnetic properties of the materials used for the cable and thus it is expected that the armouring material will also have effects on the surrounding electromagnetic field strength.

In this section, the electromagnetic fields outside the cable with different armouring materials have been simulated. Without changing the conductivity values of the armour and the electromagnetic parameters of other materials of the cable (see Table 3.1), the model uses different permeability values for the armour, i.e., $m_r = 1.0$, $m_r = 300$, $m_r = 1000$ and $m_r = 3000$. Figure 5.1 shows the simulated magnetic flux density in these cases (the field strength scales for each sub-figures (a)-(d) are identical).

The following relationship is apparent; as the permeability of the armour increases the resultant electromagnetic field strength outside the cable decreases. This can be explained by the fact that with higher permeability values, the eddy currents induced in the armour and sheaths due to the changing B-fields become higher and, in turn, give rise to stronger back EMF in the cable. Consequently, the resultant B-fields in the medium embedding the cable are decreased and so are the E-fields.

The simulation results indicate that using armour materials with higher permeability values can help to reduce the electromagnetic fields outside the submarine cable (Figure 5.1).

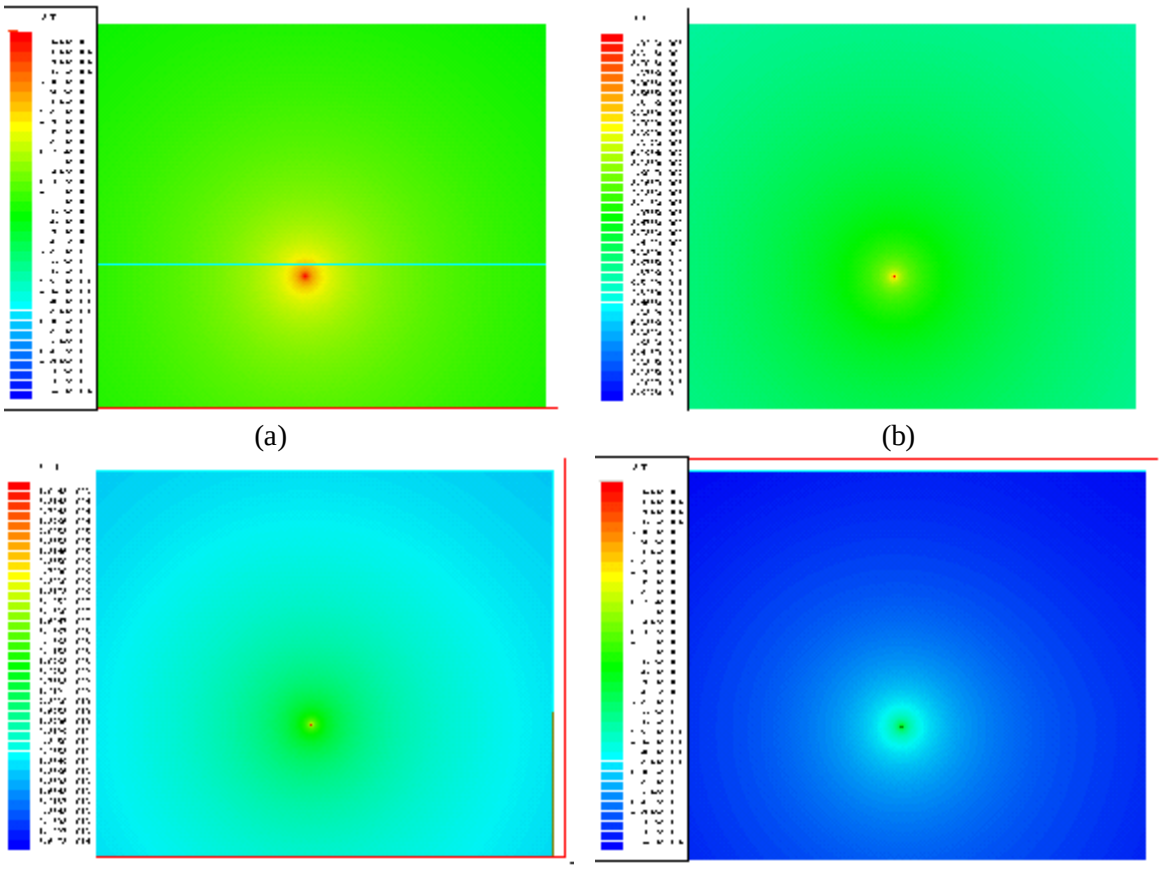

Figure 5.1: Magnitudes of the magnetic flux density outside the cable using armouring with different permeability values: (a) $m_r = 1.0$ *; (b)* $m_r = 300$ *; (c)* $m_r = 1000$ *and (d)* $m_r = 3000$
(Geometrical dimension of the simulation is as given in Figure 3.3

Figure 5.2 shows the relationships between simulated magnetic flux density and current density in the seawater with distance from the cable for armour with the four different permeability values. The distance is measured as the spatial separation between the observation point and a point at the seabed level, both being above the cable. One indication given by Figure 5.2 is that the effects of the armouring material on the magnetic and induced E-fields in the seawater are non-linear. To illustrate this further, the magnetic flux density and current density measured at 1 m above the seabed level with respect to the permeability of the armour are shown in Figure 5.3. From the equations given in section 4.7 the induced E-field decreases from approximately 1000μV/m for permeability value $m_r = 1.0$, to 0.021μV/m for permeability value $m_r = 3000$.

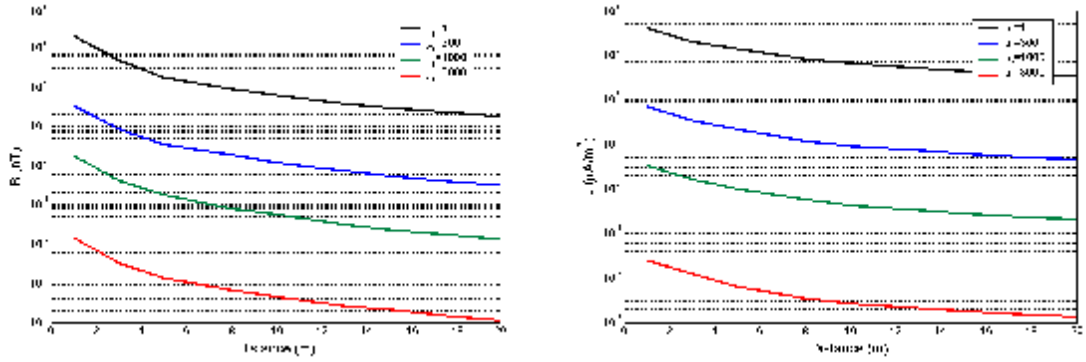

(a) (b)

Figure 5.2: Changes in the magnetic flux density (a) and current density (b) with distance from the cable using armours with different permeability values.

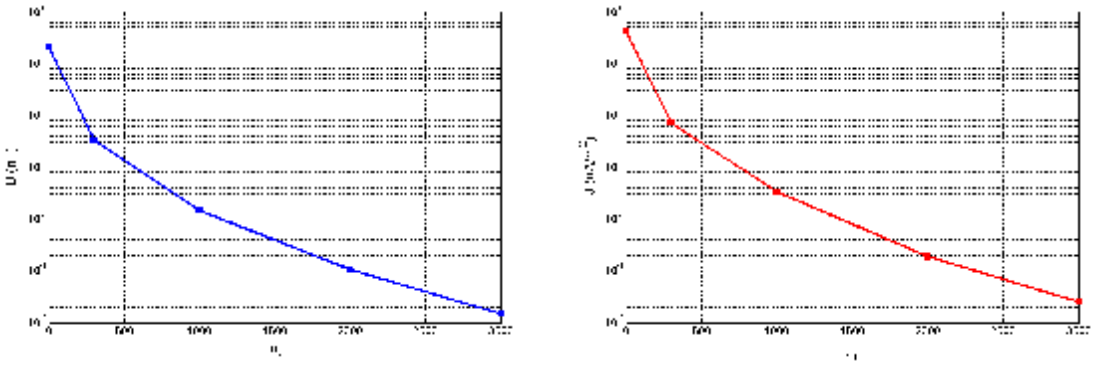

(a) (b)

Figure 5.3: The effect of different cable armour permeability on the magnetic flux density (a) and current density (b) in the seawater at 1m above the seabed level.

Summary

The simulation considered the permeability of cable armour and found the relationship that as the permeability of the armour increased the resultant electromagnetic field strength outside the cable decreased. This indicates that using materials with higher permeability values for armouring of submarine power cables can help to reduce the electromagnetic fields generated.

5.2. EFFECTS OF CONDUCTIVITY OF THE CABLE SHEATH AND ARMOUR

By analogy to the effects of permeability of the armour on the electromagnetic fields outside the cable, it is expected that changes in the conductivity values of the sheath and armour will also have an effect. In this section, the effects of different conductivity values for the sheath and armour on the surrounding electromagnetic fields have been simulated.

Without changing the permeability values of the armour and sheath and the electromagnetic parameters of other materials (see Table 3.1), the model uses conductivity values of both the sheath and armour at 50%, 10% and 1% of the original values listed in Table 3.1. These original values were referred to reference data and denoted as s_{ref}. Figure 5.4 shows the simulated magnetic flux density and current density in the seawater in these cases. As the conductivity decreases, the resultant electromagnetic field strength in the seawater increases (Figure 5.4). This can also be explained by the fact that with higher conductivity value, stronger back EMF will exist in the cable, consequently the resultant B-fields are decreased in the seawater and so are the E-fields. The simulation results also indicate that using materials with higher conductivity values as the sheath and armouring of the cable can help to reduce the electromagnetic fields outside the submarine cable.

Figure 5.5 shows the simulated magnetic flux density and current density in the seawater for different electrical sheath and armouring materials at 1m above the seabed level. A clear decreasing, linear relationship exists between the field strength and the conductivity of the sheath and armour. This is consistent with the analysis of Voitovich & Kadomskaya [12], who showed that for a close-laid three-phase cable the longitudinal current density and B-field intensity near the cable are decreased with the overall conductivity of the shield and armour.

From the equations in section 4.6, the calculated induced E-field decreases from approximately 60μV/m for 1% of s_{ref}, to 17.5μV/m for the reference conductivity (s_{ref}).

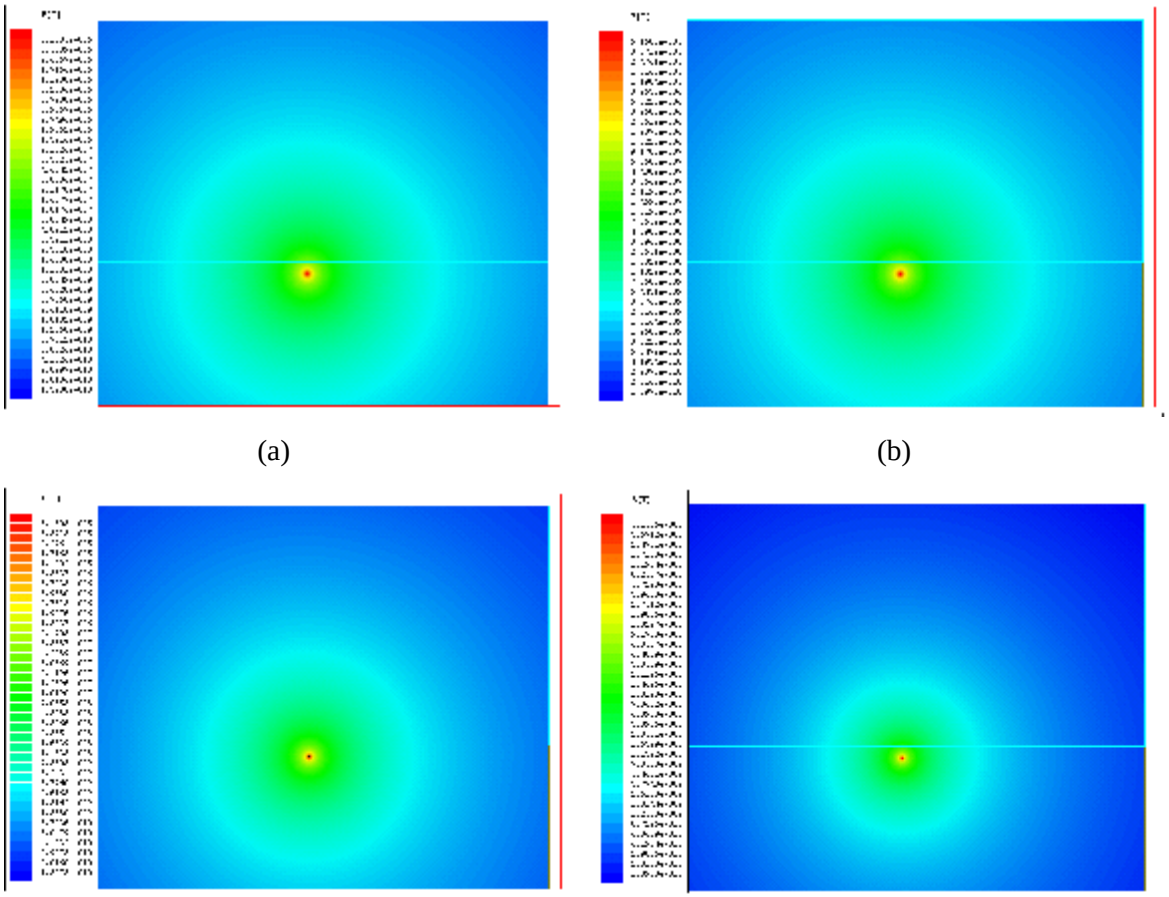

(a) (b)

(c) (d)

Figure 5.4: Magnitudes of the magnetic flux density outside the cable using the sheath and armour with different conductivity values (compared to the reference values in Table 3.1): (a) $s = 1\%$ *; (b)* $s = 10\%$ *; (c)* $s = 50\%$ *and (d)* $s = 100\%$ *.(Geometrical dimension of the simulation is as given in Figure 3.3)*

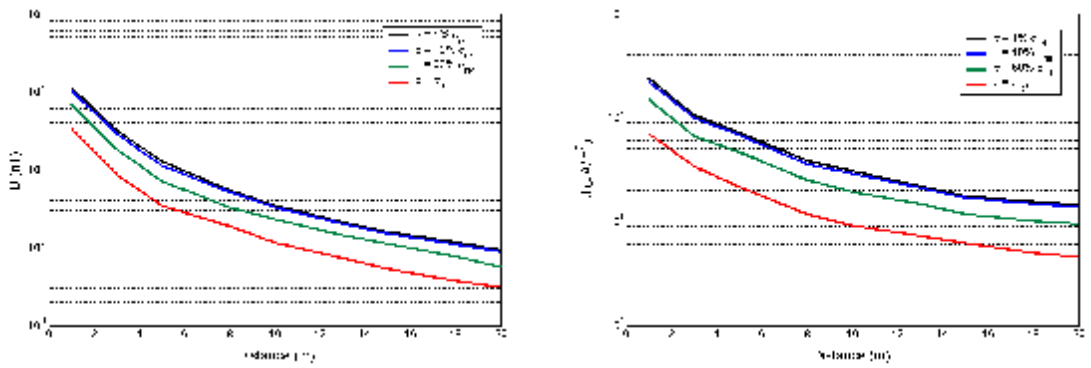

(a) (b)

Figure 5.5: The changes in magnetic flux density (a) and current density (b) with distance from the cable using sheaths and armours with different conductivity values.

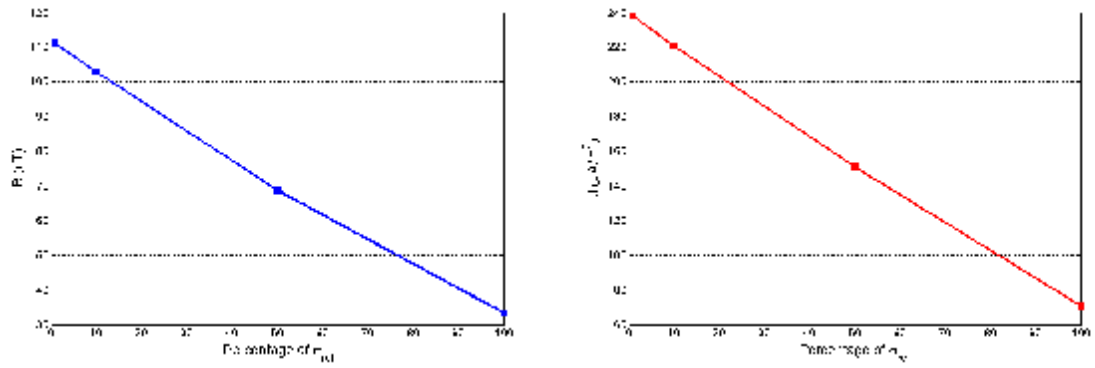

(a) (b)

Figure 5.6. : The effect of different cable sheath and armour conductivity on the magnetic flux density (a) and current density (b) in seawater at 1m above the seabed level.

Summary:

The simulation considered the conductivity of cable sheathes and armour and found that as the conductivity of the sheath and armour increased the resultant electromagnetic field strength outside the cable decreased. This indicates that using thicker sheaths or materials with higher conductivity values for the sheathing and armouring of submarine power cables can help to reduce the electromagnetic fields generated.

5.3 EFFECTS OF CABLE BURIAL

The modelling carried out in Section 3, described how a perfectly shielded cable can still generate a B-field in the local environment and that the B-fields at the same distance to the cable are similar, whether the observation point is in the seawater or in a non-magnetic seabed. Continuous B-fields are present across the boundary between the seawater and the sea sand as neither seawater or sea sand have magnetic properties (see Fig 3.7), i.e. within the parameters of the model the sediment type in which the cable is buried has no effect on the magnitude of B-field generated as long as the sediment has non-magnetic properties.

The modelling carried out in Section 3 also identified induced E-fields generated by the B-fields. The effect of cable burial to 1m on these induced E-fields is apparent in Figure 5.7.

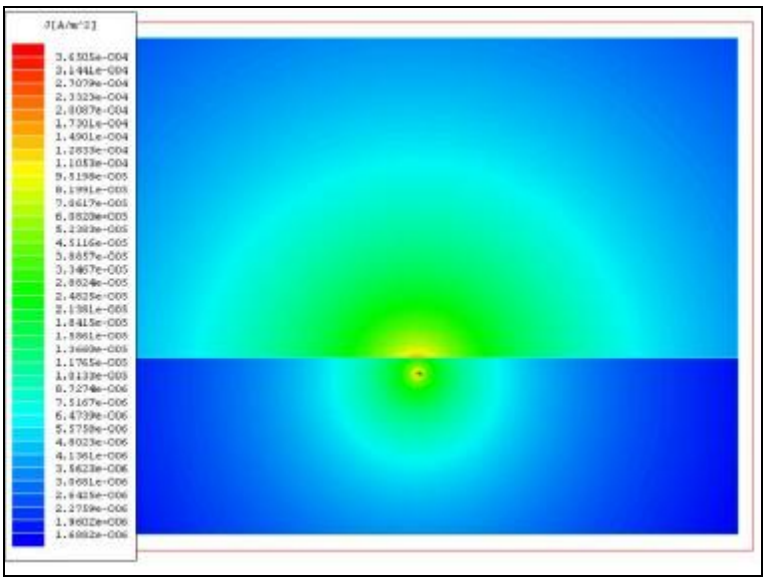

Figure 5.7: Magnitude of the current density outside the cable
(Geometrical dimension of the simulation is as given in Figure 3.3)

As the B-fields are unaffected by burial, they will induce E-fields both in the sediment and in the sea water. However, as sea water has a higher conductivity than the sediment the induced E-fields will be higher in the sea water than in the surface sediment as shown in Figure 5.7. For cables buried in sediments with lower conductivity the induced E-field will be lower than shown in Figure 5.7 but only in the sediment, this will not apply to the sea water. However, if the sea water changes in conductivity (eg. in an estuary) then the induced E-fields in the water would be expected to changes. This scenario needs further investigation to fully understand the consequences of salinity changes and the associated

tidal and current effects on the resultant EMFs. Although the burial of a cable will not effectively mitigate against B-fields and induced E-fields if it is buried to the suggested 1m depth then it is likely to reduce exposure of electromagnetically sensitive species to the strongest EMFs that exist at the 'skin' of the cable owing to the physical barrier of the substratum.

5.4 CONCLUSIONS CONCERNING MITIGATION

There is a decreasing, non-linear relationship between electromagnetic field strength and permeability of the armouring material used in the cable. Additionally, a decreasing, linear relationship exists between electromagnetic field strength and the conductivity of the materials. This indicates that a reduction in the strength of the electromagnetic fields induced by a three-phase 132kV XLPE submarine cable can be achieved through the application of materials with high conductivity and high permeability. In fact at very high permeability values the induced E-fields are less than the lowest known electrical emission that elasmobranchs are sensitive to[1] (see Section 6.0). According to existing knowledge producing cables with these high permeability values would require more specialised materials and manufacturing process and would also require an understanding of their other electrical properties (e.g. conductivity). These results provide useful information for optimising the future design and manufacture of submarine cables, to reduce electromagnetic field emissions.

Whilst burial in any non-magnetic sediment is ineffective in 'dampening' a B-field, cable burial to a depth of at least 1m is likely to provide some mitigation for the possible impacts of the strongest B-fields and induced E-fields that exist within millimetres of the cable, on electrosensitive species, owing to the physical barrier of the substratum. Burial to greater depths will have a negligible effect on the B-field emitted.

On the assumption that the same power (= voltage x current) is transmitted at a higher voltage, e.g. 132kV instead of 33kV (a factor of 4 increase), then the current in the cable could be reduced by a factor of 4. As a consequence the induced E-field would decrease also by a factor of 4. Therefore, another option is to use a substation to convert the voltage from 33kV to 132kV could be used to reduce the current carried by a cable and the induced E-fields. In theory, this would add to mitigation of the EMF effects of sending power to the shore but practical and economic considerations would also need to be taken into account.

6. CONSIDERATION OF THE RESULTS WITH RESPECT TO FISH SENSITIVE TO ELECTROMAGNETIC FIELDS

In the CCW commissioned report, Gill & Taylor[1] highlighted through a review of the literature and subsequent experimentation that elasmobranchs were sensitive to E-fields ranging from 5nV/cm - 10μV/cm (0.5 - 1000 μV/m), with species specific ranges likely to occur within this full range. Throughout most of the range of E-fields the elasmobranchs would be expected to be attracted to the source. At the higher field levels of 1μV/cm or greater the fish would be expected to avoid the source of the emission. In this context the results of the modelling and *in situ* measurement of EMF from subsea power cables can be assessed.

6.1. RESPONSE TO ELECTRIC FIELDS

The most important result is that the magnetic field emitted by an industry standard, three-core power cable will induce electric fields. In the case modelled this resulted in a predicted E-field of approximately 91μV/m (=0.91μV/cm) on the seabed adjacent to a cable buried to 1m. This level of E-field is on the boundary of emissions that are expected to attract and those that repel elasmobranchs. In addition, the induced E-fields calculated from the B-fields measured *in-situ* were also within the lower range of detection by an elasmobranch.

The model of induced E-fields from a buried cable showed that the field would dissipate relatively rapidly with distance away from the longitudinal axis of the cable. However, even at 20m from the cable (horizontally along the seabed or vertically in the water column) the E-field would remain within the range of sensitivity of an elasmobranch; therefore a dogfish (or another species with similar sensitivity) may be able to detect a buried cable within a number metres of the cable. Further studies are therefore required to specifically address the question of whether the elasmobranchs can detect these E-fields.

An important aspect of cable burial is that the exposure of electro-sensitive species to the strongest induced E-fields generated by the B-field surrounding the cable would be limited by the physical barrier of the substratum. Although some elasmobranchs use digging activity to uncover prey this occurs in the surface layers of the substratum. Hence burial should reduce the exposure of electrosensitive fish to the largest induced E-fields thereby reducing the potential for an avoidance response.

The model of cables with non-perfect shielding showed that although leakage E-fields would occur their intensity would be less than the induced field. As the induced fields would predominate we would not predict any further effect on the fish.

The options for mitigation using either change in permeability or conductivity indicate that the induced E-field can be effectively reduced. In the case of increased permeability the higher values reduced the E-field to less than the lowest detectable emission currently known. For increased conductivity the E-field emission although reduced still remains within the lower range of detection of elasmobranchs. Hence increased permeability and conductivity of the cable would minimise the potential for an avoidance reaction by a fish if it encountered the E-field, but unless permeability is very high there may still be an attraction response.

Another important consideration is the relationship between the amount of cable, either buried or on the seabed surface, producing induced E-fields and the available habitat of an electrosensitive species. Inter-turbine cabling, which connects all the turbines together, may be laid on the seabed. If this is the case then the number of turbines and their proximity to each other will define the size of the area within which the cabling will be on the substratum. The type of substratum that the turbines are constructed on represents a marine habitat that will have particular species associated with it even if only at some stage of their life history. Therefore the extent of the habitat and the amount taken up by the cabling emitting induced E-fields may have important consequences for any electrosensitive species. In addition, as the number of turbines increases (either through more individual windfarms or larger developments) there may be implications for these species.

Just as human hearing distinguishes many sound sources, fish must discriminate between prey and the E-fields induced by water currents in the earth's B-field. A small number of studies indicate that the discriminatory ability of electrosensitive fish is not only a function of the size of the E-field emitted but is also linked to the frequency of the emission. Furthermore, it has been shown in laboratory studies that in a few species of fish (mainly species of passively electroreceptive elasmobranchs) the sensitivity to E-fields reduces at frequencies approaching 10 Hz[17] whereas other fish (particularly actively electroreceptive fish) can detect and also generate high frequency pulses[18]. According to current understanding, the majority of the electrosensitive species in UK coastal waters are elasmobranchs[1] (see Appendix III), and most of the species use passive electro-detection. There are only two species (*Torpedo* sp.) that can actively generate E-fields as well as detect them[1]. No information exists on the range of frequencies of E-fields that UK species can detect. It is therefore important to determine if the power cable operating frequency (50Hz) and associated sub-harmonic frequencies have any effect on the EMFs that are detectable by UK electrosensitive fishes.

6.2. RESPONSE TO MAGNETIC FIELDS

The magnetic fields, both modelled and measured, from sub-sea power cables were well below the earth's background geomagnetic field. However, it should be noted that the small, time varying B-field emitted given by the model may be perceived differently by sensitive marine organisms compared to the persistent, static geomagnetic field generated by the Earth. The few studies that have looked at the potential effects of the emitted B-fields suggest that migratory fish do not deviate from their normal migration path[8,9]. However, these experiments considered a B-field generated by a high-voltage direct current subsea cable. The response of fish to a small B-field generated by an alternating current is unknown. Some elasmobranchs are able to directly sense changing B-fields (around 2000 μT/sec) [17]. Such fish may therefore be able to detect B-fields at a power frequency (50 Hz) of around 6 μT_{RMS} (or 5 A/m). If this hypothesis were correct then these fish would be able to detect the B-fields around non-armoured power cables and possibly armoured power cables.

7. RECOMMENDATIONS FOR FURTHER STUDIES

As the measurements at Rhyl clearly indicate, the ***in-situ*** EMF generated by subsea power cables is far more complex than either a simple model or laboratory test can predict. However, the approach of modelling and parallel studies of EMF ***in situ*** demonstrates that our knowledge can be significantly improved through combining studies. In addition, by considering specific biological implications of the results we have been able to put the results into greater environmental context. We advocate that the same approach should be applied to the following future studies:

7.1. ELECTRICAL ENGINEERING STUDIES

- A clearer understanding of the mechanisms leading to the induction of E-fields in seawater and estuaries and possible solutions for reducing the effect.
- Quantify sub-harmonic frequencies and amplitudes of the induced emissions.
- Monitoring of EMF from phase 1 offshore windfarm subsea power cables ***in situ*** using suitable magnetic and E-field sensors.
- Mapping of EMF in real case scenarios to determine temporal variability in emissions.
- A more advanced model to describe the interactions of EMF, direct or induced, from power cables in the marine environment.
- Modelling of real cable situations and verification of the predicted results by site tests.
- Development and testing of new specification sub-sea cables (e.g. using materials with different permeability and conductivity values).
- Cost-benefit analyses of using different cabling configurations, cable burial and sub-stations.
- Laboratory measurements of E- and B-fields in fish populated tanks.

7.2. BIOLOGICAL STUDIES

Clearly, the interaction of the induced E-fields with electrosensitive fish needs to be investigated. More specifically:

- Behavioural studies of whether there is a response (attraction or avoidance) particularly by benthic electrosensitive fish to encounter with induced E-fields from buried and unburied cables. These studies need to consider these responses in relation to specific life history stages (eg. juveniles), sex related and individual variability and whether there are any implications at the population level (eg. use of habitat or food finding ability by species groups).

- Species-specific studies to determine the potential degree of response of different UK species to EMF from subsea power cables. Again the focus should be on the implications at population level.
- Consideration of variability in B-fields and their potential impact on magneto-sensitive species (specifically cetaceans, migratory teleost fishes and elasmobranchs).
- Analysis of the extent of coastal marine habitat used by UK electrosensitive species, particularly those of fisheries concern, in relation to the area of seabed allocated to windfarm developments.
- A scientifically rigorous survey program for new windfarm developments, which consider the species number, abundance and distribution in relation to habitat availability. Surveys should focus on mortality, immigration/emigration and recruitment rates and also consider philopatry (the tendency of organisms to remain in or migrate between home areas).

Important note: laboratory behaviour studies will require UK Home Office licensing according to the Animals (Scientific Procedures) Act 1984.

8. OVERALL CONCLUSIONS

A review of present offshore windfarm cabling strategies highlighted a number of factors need to be taken into consideration such as utility connection voltage, sub-sea cable technology, turbine electrical design and distance from shore. In addition, the function of inter-turbine cables is also affected by a number of factors namely cable voltage, sizing, armour and burial. However, the current state of knowledge regarding the EMF emitted by the power cables, based on an assessment of existing publications and personal communications, is too variable and inconclusive to make an informed assessment of any possible environmental impact of EMF in the range of values likely to be detected by organisms sensitive to electric and magnetic fields. Therefore, modelling and direct measurement of the electric and magnetic field components of EMF was undertaken.

An Alternating Current (AC) Conduction Field Solver model and Eddy Current Field Solver model were used within the 'Maxwell 2D' software program which allows the simulation of electromagnetic and electrostatic fields in structures with uniform cross-sections by solving Maxwell's equations using the finite-element method. The modelling was based on EMF generated by a 132kV XLPE three-phase submarine cable designed by Pirelli. For a cable modelled with perfect shielding:

- The model showed that the cable did not directly generate an E-field outside the cable.
- However, B-fields generated by the cable created 'induced' E-fields outside the cable, irrespective of shielding.
- Maxwell's Eddy Current Field Solver model showed that B-fields are present in close proximity to the cable and that the sediment type in which a cable is buried has no effect on the magnitude of B-field generated.
- The magnitude of the B-field on the 'skin' of the cable (i.e. within millimetres) is approximately 1.6μT which will be superimposed on any other B-fields (eg. earth's geomagnetic field).
- The magnitude of the B-field associated with the cable falls to background levels within 20m.

For a cable modelled with non-perfect shielding/earthing

- An E-field is generated outside the cable.
- This additional E-field is smaller than the normal induced E-field and decreases with the distance from the cable.

To directly measure the electromagnetic emissions from undersea cables two sensors were developed to detect electric and magnetic fields. The sensors were calibrated and tested in the laboratory and then tested *in situ* near to a three-phase AC power cable in seawater.

- Both magnetic and electric fields were detected.
- The B-field sensor developed performed well in the laboratory and site trials. It was able to detect B-fields down to 0.5 nT $_{RMS}$.
- The B-field level measured during site trials (56 nT $_{RMS}$) closely matched levels predicted by modelling. This validated the model used for B-field calculations.
- Tests in the seawater tank in the laboratory showed that the E-field measured does not vary significantly with the shape of the sensor. This result implies the E-field in the water can be calculated from the current density using the following equation:

$$\text{Electric field } (\mu V/m) = \frac{1000000 \bullet \text{Current density } (A/m^2)}{\text{Conductivity (siemens/m)}}$$

$$= \frac{10000 \bullet \text{Current density } (mA/m^2)}{\text{Conductivity (milli-siemens/cm)}}$$

(For seawater the salinity/conductivity is approximately 4 S/m or 40 mS/cm)

- Modelling predicted that the B-field observed during field trials would induce an electric current density in the seawater of 0.1 mA/m² when the cable is buried at a depth of 1m. It therefore follows that the induced E-field in the water would be around 25 μV/m.
- Tests performed on a mock power cable indicated that with no armour or shield the B-field outside the cable was very high at approximately 1000 μT $_{RMS}$. This was a similar level to that predicted for single-phase power cables.
- The low input impedance E-field sensor developed had sensitivity comparable to that of electro-sensitive fish. During site trials this sensor detected a large E-field (above 70 μV/m) sufficient to overdrive the sensor.
- A contributory factor to this field may have been the lack of steel armour in the 33kV cable at Rhyl. However, this fact does not completely account for the large E-field detected at a distance of approximately one kilometre from the cable. Time limitations did not allow further investigation of the detected field.
- High input impedance E-field sensors tend to be sensitive to sound; therefore producing a sensor with sufficient sensitivity for this application (i.e. low output noise) would be difficult and requires further work.
- A method is given for calculating the induced E-field around a low frequency (such as 50 Hz) AC power cable due to the emanating B-field. This method requires ***in situ*** measurement of the B-field generated by an operational cable.

To consider mitigation, the models simulated changes in permeability of the power cable armour and conductivity of the cable sheath and armour.

- A negative, linear relationship was found between electromagnetic field strength and the conductivity of the materials used in the cable. Additionally, a negative, non-linear relationship was found between electromagnetic field strength and permeability of the armouring material. This indicates that a reduction in the strength of the electromagnetic fields induced by a three-phase 132kV XLPE submarine cable can be achieved through the application of materials with high conductivity and high permeability
- These results provide useful information for the design and manufacture of submarine cables with reduced EMF emissions
- Burial was shown to be ineffective in 'dampening' a B-field, however cable burial to a depth of at least 1m is likely to provide some mitigation for the possible impacts of the strongest magnetic and induced electrical fields that exist within millimetres of the cable owing to the physical barrier of the substratum to electro-sensitive species. Burial to greater depths will have a negligible effect on the B-field emitted.
- Using the assumption that delivery of electric power remains the same, an increase in voltage from 33kV to 132kV, for example, would mean a reduction in current by a factor of four. As the induced E-field is related to the cable current this means that the induced E-field would also be four times less given the same environmental conditions and cable. Transmitting power at a higher voltage and lower current could be used to add to mitigation of the EMF effects of sending power to the shore

In terms of the potential significance of the modelled results to electrosensitive fish the following conclusions were made:

- EMF emitted by an industry standard three-core power cable will induce E-fields.
- In the case modelled this resulted in a predicted E-field of approximately 91μV/m (=0.9 μV/cm) at the seabed adjacent to a cable buried to 1m. This level of E-field is on the boundary of E-field emissions that are expected to attract and those that repel elasmobranchs.
- In addition, the induced E-fields calculated from the B-fields measured *in-situ* were also within the lower range of detection by an elasmobranch.
- The options for mitigation using either changes in permeability or conductivity indicate that the induced E-fields can be effectively reduced, however, unless very high permeability materials are used in the cable these E-fields are still within the lower range of detection of elasmobranchs. Hence any reduction in E-field emission would minimise the potential for an avoidance reaction by a fish if it encountered the field but may still result in an attraction response

- Another important consideration is the relationship between the amount of cable, either buried or on the seabed surface, producing induced E-fields and the available habitat of electrosensitive species.
- The is also a need to determine if the power cable operating frequency (50Hz) and associated sub-harmonic frequencies have any effect on the EMFs that are detectable by UK elasmobranchs.

A number of further studies are identified, which are required to fully understand the interaction of the B-fields and induced E-fields with electrosensitive fish.

9. REFERENCES

1. Gill, A.B. & Taylor, H. (2002) The potential effects of electromagnetic fields generated by cabling between offshore wind turbines upon elasmobranch fishes. Report to the Countryside Council for Wales (CCW Contract Science Report No 488) 60 pages.

2. King, S. Y. & Halfter, N. A. (1982). *Underground Power Cables*, New York: LongMan Inc.

3. King, P. Personal communication regarding electromagnetic fields generated by windfarm cabling. (Pirelli Cables).

4. Smith, A. Personal communication regarding electromagnetic fields generated by windfarm cabling (AEI Cables Ltd.).

5. Bochert, R. Personal communication regarding electromagnetic fields generated by windfarm cabling (Institut für Ostseeforschung Warnemünde, Germany).

6. Mikkelson, S.D. Personal communication regarding electromagnetic fields generated by windfarm cabling (Eltra, Denmark).

7. Danish Institute for Fisheries Research (2002). Effects of marine windfarms on the distribution of fish, shellfish and marine mammals in the Horn's Rev area. Report to Elsamprojekt A/S, (Background Report No 24) 42 pages.

8. Westerberg, H & Begout-Anras, M.L. (2000) Orientation of silver eel (Anguilla anguilla) in a disturbed geomagnetic field. Advances in Fish Telemetry. Proceedings of the Third Conference on Fish Telemetry in Europe, Norwich, England, June 1999. Eds. Moore, A. & Russel, I. CEFAS Lowestoft.

9. Westerberg, H. (2000) Effect of HVDC cables on eel orientation. In Merck, T & von Nordheim, H (eds). *Technishe Eingriffe in marine Lebensraume*. Published by Bundesamt fur Naturschutz.

10. Bio/consult AS. (2002) Possible effects of the offshore windfarm at Vindeby on the outcome of fishing. Report to SEAS, Denmark. 23 pages.

11. Holm Skyt, P. Personal communication regarding EMF generated by offshore windfarm cabling (SEAS, Denmark).

12. Voitovich, R. A. & Kadomskaya, K. P. (1997). Influence of the Design Parameters of High-Voltage Underwater Power Cables on the Electromagnetic Field Intensity in an Aqueous Medium. *Electrical Technology*, No. 2, PP. 11-21, 1997

13. May, A. (2002). Submission on the' Response by Basslink Pty Ltd to the Draft Report on the Basslink Joint Advisory Panel (submission 2 of 3), Proposed Metallic Return.

14. http://www.pirelli.com/en_42/cables_systems/energy/product_families/pdf/leaflet_subsea.pdf

15. The Ansoft Designer Ltd. Website (http://www.ansoft.com)

16. Karus, J. D. (1991). *Electromagnetics*, New York: McGraw-Hill.

17. Brown, H.R., Andrianov, G.N. & Ilyinsky, O.B. (1974). Magnetic Field perception by electroreceptors in Black Sea skates. *Nature*, Vol. 249, No 5453, pp 178-179.

APPENDIX 1: CONSULTATION

Organisation	**Contact**
DMU/NERI, Denmark	Oluf Henriksen
Fiskeriverket (Dept Fisheries), Sweden	Dr. Hakan Westerberg
Deutsche Energie Agentur, Germany	Mr. Tiedemann
Institut für Ostseeforschung Warnemünde, Germany	Dr. M. Zettler
Institut für Ostseeforschung Warnemünde, Germany	Dr. Ralf Bochert
SEAS Wind Energy Centre, Denmark	Pernille Holm Skyt
Vindkompaniet Öland, Sweden	Staffan Niklasson
Scottish & Southern (S+S)	Dave Telford
Pirelli Cables	Phil King
AEI Cables Ltd.	Max Livigni
AEI Cables Ltd.	Alan Smith
ABB Power Technology Products	Ove Tollerz
Seascape Energy	Adrian Maddocks
National Wind Power	David Bean
Offshore Energy Resources Ltd	Dan Badger
Norfolk Offshore Wind	David Linley
NEG Micon	Peter Clibbon
Eltra	Dr Soren Damsgaard Mikkelsen
University of the Witwatersrand	Prof George J Gibbon
KEMA	R. Smeets
Shell	J. Bannell
NGC	I. Glover
P B Power	G. Ali
Doble	A.Wilson
NGC (CIGRE)	M. Waldron
Consultant	D. Proctor
Northwest Utilities	J. Walker
ETSU/EA Technology	H. Tonge
Power Systems	Shaun Preston
Hydrocables Systems Ltd	Rick Gill
SPOK Aps, Denmark	Dr Hans Christian Sorensen
ERA Technology	Mark Cotes
EA Technology	Stephanie Holmes

APPENDIX II: CIRCUIT DIAGRAMS

1. MAGNETIC FIELD SENSOR

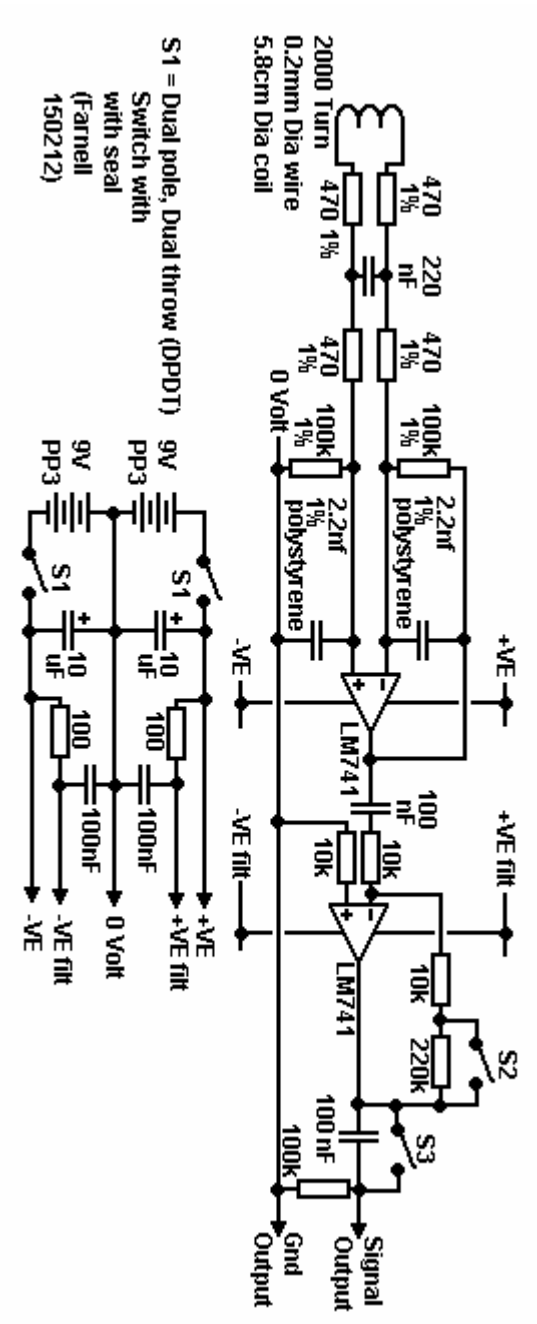

2. HIGH IMPEDANCE ELECTRIC FIELD SENSOR

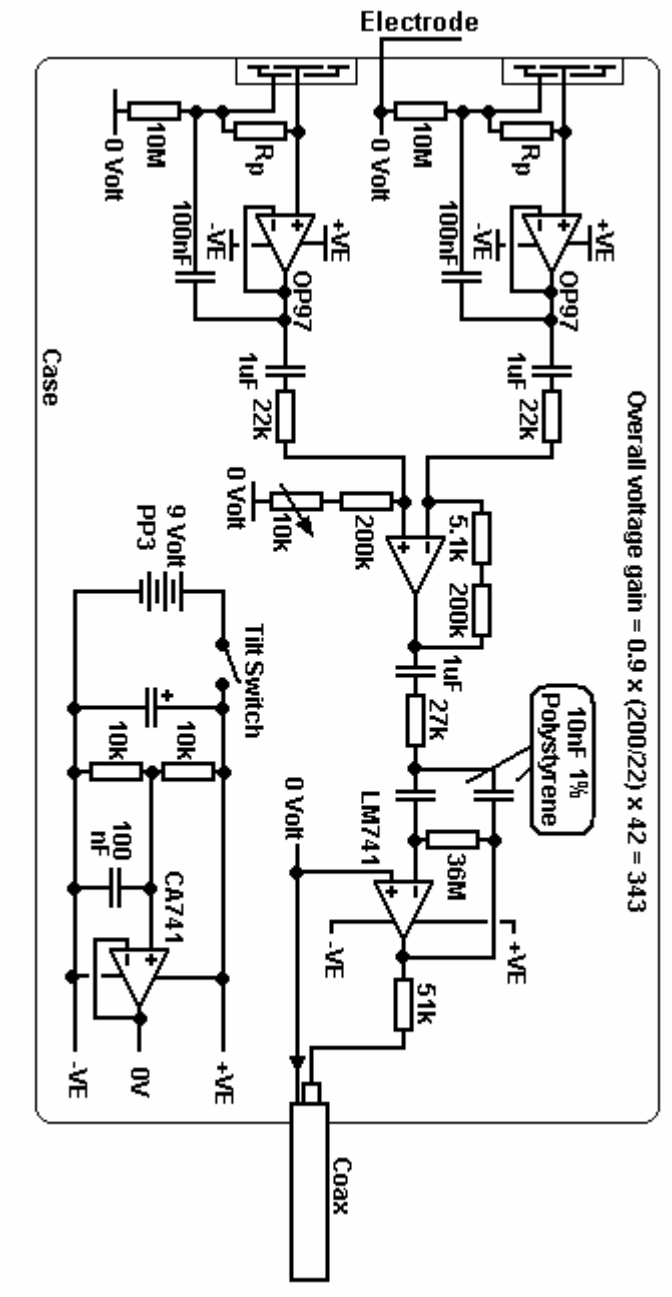

Rb = parasitic resistance between the electric field guard ring and the 4mm² Electrode (Around 18000 MΩ)

3. LOW IMPEDANCE ELECTRIC FIELD SENSOR

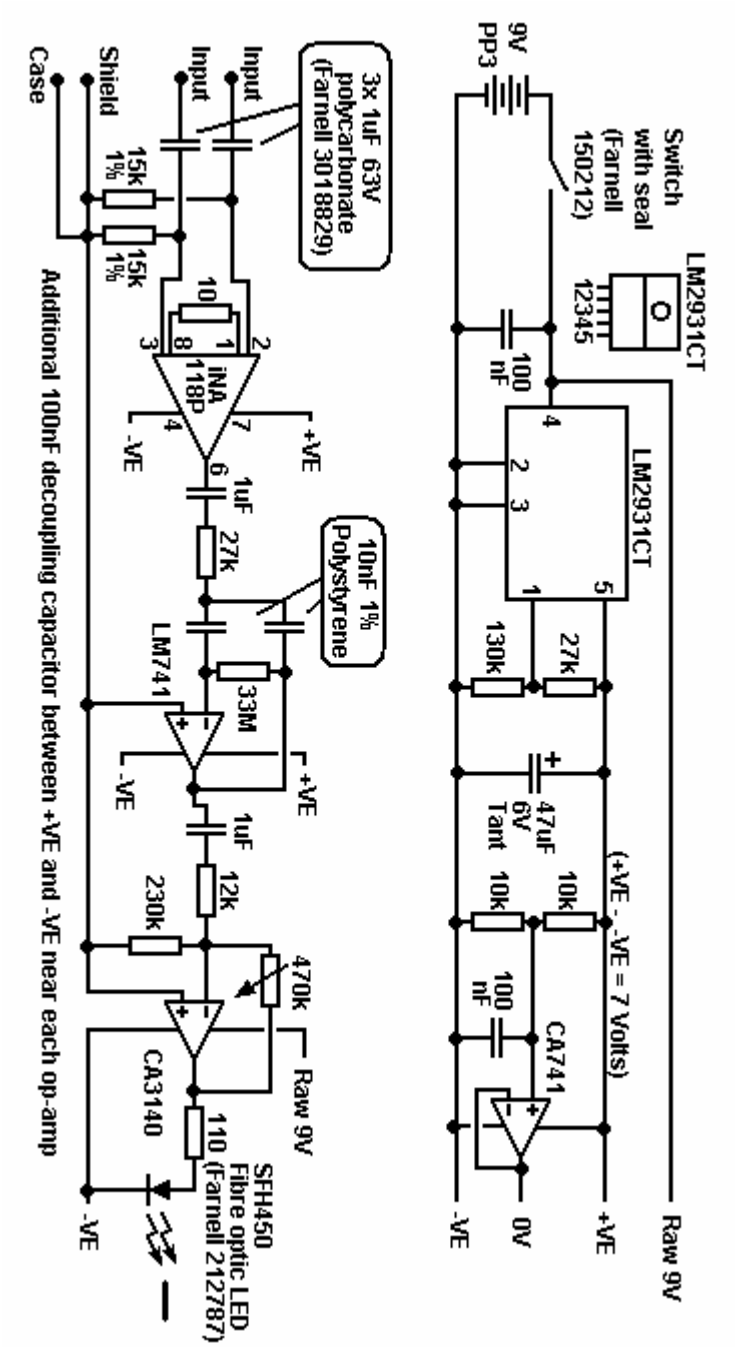

APPENDIX III: SPECIES LIST OF KNOWN ELECTRORECEPTIVE FISHES IN UK COASTAL WATERS.

Species	Common name	Order	Family	Common grouping
Elasmobranchii (Sharks)				
Alopias vulpinus	Thintail thresher	Lamniformes	Alopiidae	Thresher sharks
Centrophorus squamosus	Leafscale gulper shark	Squaliformes	Centrophoridae	
Centroscyllium fabricii	Black dogfish	Squaliformes	Dalatiidae	Sleeper sharks
Cetorhinus maximus	Basking shark	Lamniformes	Cetorhinidae	Basking sharks
Chlamydoselachus anguineus	Frilled shark	Hexanchiformes	Chlamydoselachidae	Frilled sharks
Dalatias licha	Kitefin shark	Squaliformes	Dalatiidae	Sleeper sharks
Deania calcea	Birdbeak dogfish	Squaliformes	Centrophoridae	
Echinorhinus brucus	Bramble shark	Squaliformes	Echinorhinidae	Bramble sharks
Etmopterus spinax	Velvet belly lantern shark	Squaliformes	Dalatiidae	Sleeper sharks
Galeorhinus galeus	Tope shark	Carcharhiniformes	Triakidae	Houndsharks
Galeus melastomus	Blackmouth catshark	Carcharhiniformes	Scyliorhinidae	Cat sharks
Heptranchias perlo	Sharpnose sevengill shark	Hexanchiformes	Hexanchidae	Cow sharks
Hexanchus griseus	Bluntnose sixgill shark	Hexanchiformes	Hexanchidae	Cow sharks
Isurus oxyrinchus	Shortfin mako	Lamniformes	Lamnidae	Mackerel sharks, white sharks
Lamna nasus	Porbeagle	Lamniformes	Lamnidae	Mackerel sharks, white sharks
Mustelus asterias	Starry smooth-hound	Carcharhiniformes	Triakidae	Houndsharks
Mustelus mustelus	Smooth-hound	Carcharhiniformes	Triakidae	Houndsharks
Oxynotus centrina	Angular roughshark	Squaliformes	Dalatiidae	Sleeper sharks
Prionace glauca	Blue shark	Carcharhiniformes	Carcharhinidae	Requiem sharks
Scyliorhinus canicula	Small-spotted catshark	Carcharhiniformes	Scyliorhinidae	Cat sharks
Scyliorhinus stellaris	Nursehound	Carcharhiniformes	Scyliorhinidae	Cat sharks
Scymnodon obscurus	Smallmouth velvet dogfish	Squaliformes	Dalatiidae	Sleeper sharks
Scymnodon squamulosus	Velvet dogfish	Squaliformes	Dalatiidae	Sleeper sharks
Somniosus microcephalus	Greenland shark	Squaliformes	Dalatiidae	Sleeper sharks
Sphyrna zygaena	Smooth hammerhead	Carcharhiniformes	Sphyrnidae	Hammerhead, scoophead shark
Squalus acanthias	Piked dogfish	Squaliformes	Squalidae	Dogfish sharks
Squatina squatina	Angelshark	Squatiniformes	Squatinidae	Angel sharks

Cont/

Elasmobranchii (Skates & Rays)				
Amblyraja hyperborea	Arctic skate	Rajiformes	Rajidae	Skates
Amblyraja radiata	Thorny skate	Rajiformes	Rajidae	Skates
Bathyraja spinicauda	Spinetail ray	Rajiformes	Rajidae	Skates
Dasyatis pastinaca	Common stingray	Rajiformes	Dasyatidae	Stingrays
Dipturus batis	Blue skate/common skate	Rajiformes	Rajidae	Skates
Dipturus oxyrinchus	Longnosed skate	Rajiformes	Rajidae	Skates
Leucoraja circularis	Sandy ray	Rajiformes	Rajidae	Skates
Leucoraja fullonica	Shagreen ray	Rajiformes	Rajidae	Skates
Leucoraja naevus	Cuckoo ray	Rajiformes	Rajidae	Skates
Mobula mobular	Devil fish	Rajiformes	Myliobatidae	Eagle and manta rays
Myliobatis aquila	Common eagle ray	Rajiformes	Myliobatidae	Eagle and manta rays
Raja brachyura	Blonde ray	Rajiformes	Rajidae	Skates
Raja clavata	Thornback ray	Rajiformes	Rajidae	Skates
Raja microocellata	Small-eyed ray	Rajiformes	Rajidae	Skates
Raja montagui	Spotted ray	Rajiformes	Rajidae	Skates
Raja undulata	Undulate ray	Rajiformes	Rajidae	Skates
Rajella fyllae	Round ray	Rajiformes	Rajidae	Skates
Rostroraja alba	Bottlenosed skate	Rajiformes	Rajidae	Skates
Torpedo marmorata	Spotted torpedo	Torpediniformes	Torpedinidae	Electric rays
Torpedo nobiliana	Atlantic torpedo	Torpediniformes	Torpedinidae	Electric rays
Holocephali (Chimaeras)				
Chimaera monstrosa	Rabbit fish	Chimaeriformes	Chimaeridae	Shortnose chimaeras or ratfishes
Agnatha (Jawless fish)				
Lampetra fluviatilis	European river lamprey	Petromyzontiformes	Petromyzontidae	Lampreys
Petromyzon marinus	Sea lamprey	Petromyzontiformes	Petromyzontidae	Lampreys

Note: All species shown have been recorded in UK coastal waters at depths less than 200m.

Data sources:

Froese, R. and D. Pauly. eds. (2003). FishBase. World Wide Web electronic publication. www.fishbase.org, version 04 June 2003.

Vas, P. (1991). A field guide to the sharks of British coastal waters. Field Studies Council AIDGAP Publication No. 205.